# Chapter 9

# Oceanic basin connections®

Janet Sprintall<sup>a</sup>, Arne Biastoch<sup>b</sup>, Laura K. Gruenburg<sup>c</sup>, and Helen E. Phillips<sup>d</sup>

<sup>a</sup>Climate, Atmospheric Sciences and Physical Oceanography, Scripps Institution of Oceanography, University of California San Diego, La Jolla, CA, United States, <sup>b</sup>GEOMAR Helmholtz Centre for Ocean Research and Kiel University, Kiel, Germany, <sup>c</sup>School of Marine and Atmospheric Sciences, Stony Brook University, Stony Brook, NY, United States, <sup>d</sup>Institute for Marine and Antarctic Studies and Australian Antarctic Program Partnership, University of Tasmania, Hobart, TAS, Australia

## 1 Introduction

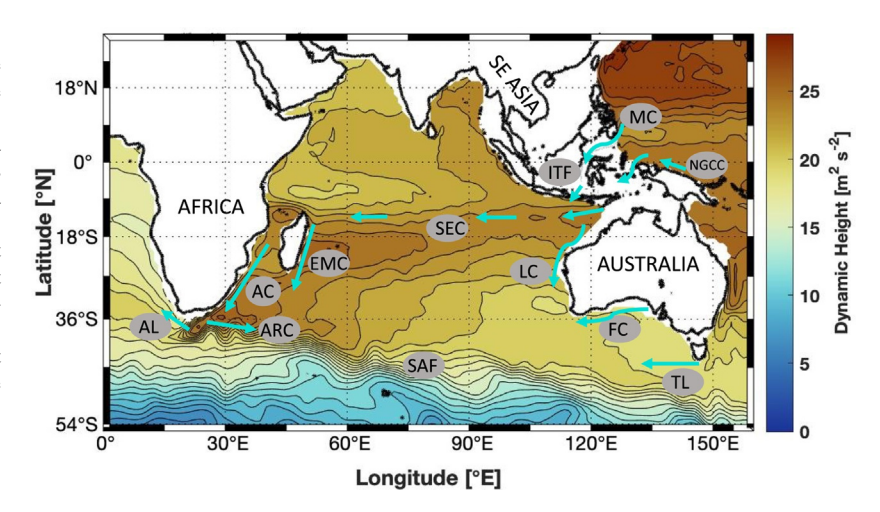
The global thermohaline circulation driven by density variations in response to variable surface heat and freshwater fluxes acts to connect the different ocean basins. Such connectivity is maintained via open boundaries around ocean borders that permit interbasin exchanges of the different water masses and their biogeochemical properties. The boundaries of the Indian Ocean basin are characterized by some unique features that distinctively set its connectivity apart from the other oceans affecting the transport of heat, freshwater, and other properties (Fig. 1).

Unlike other ocean basins, the Indian Ocean is closed off in the north by the Asian land mass. This not only limits the northern extent of the currents within the ocean basin but also results in the extreme land-sea surface temperature contrasts that control the Asian monsoon system, which is of fundamental importance for the Indian Ocean circulation (Ummenhofer et al., 2024). The Indian Ocean uniquely has a low-latitude ocean connection via the various channels of the Indonesian archipelago. Critically, this conduit provides a linkage between the warm and fresh pools of the tropical Pacific and Indian Oceans. The coastal subtropical boundary currents within the Indian Ocean also have noticeable differences compared to their global counterparts. The Leeuwin Current is the only poleward flowing eastern boundary current in the world, flowing along the Western Australian coastline to feed into a complex series of currents south of Australia. This current system influences regional climate and provides a key conveyance of many important tropical marine species and their larvae that are vital to sustaining one of Australia's largest fisheries (Caputi et al., 1996). On the other side of the basin, the Agulhas Current is the strongest western boundary current in the Southern Hemisphere, flowing poleward along the east coast of the southern African continent. Most of the Agulhas Current retroflects south of the Agulhas Bank and returns eastward, while a smaller part leaks westward into the Atlantic Ocean primarily through large eddies known as Agulhas Rings (Lutjeharms, 2006). These eddies return warm and salty Indian Ocean waters into the Atlantic and play a significant role in the upper branch of the global meridional overturning circulation (Gordon, 1986). The eastward-flowing Antarctic Circumpolar Current in the Southern Ocean marks the southern boundary of the Indian Ocean and provides direct sources for both the shallow and deep subtropical cells in the Indian Ocean circulation. South of Australia has a remarkable series of westward-flowing streams that provide inflow into the Indian Ocean north of the Antarctic Circumpolar Current. These streams include the Pacific-sourced Tasman leakage and the Flinders Current that extend into the southeastern Indian Ocean subtropical gyre. There is also some evidence that the Indian Ocean subtropical gyre is embedded in a Southern Hemisphere supergyre that broadly connects the southern Atlantic, Indian, and Pacific Ocean subtropical gyres (Speich et al., 2002, 2007; Ridgway & Dunn, 2007).

The interbasin exchanges thus play a critical role in the transportation of oceanic properties that sustain our unifying view of a single, vast, interconnected global ocean circulation. This chapter examines our knowledge of interocean exchanges with the Indian Ocean from observational evidence and numerical simulations. Section 2 highlights the tropical interbasin connection from the Pacific, addressing the pathways and variability of the Indonesian Throughflow (ITF) and its relative influence on the Indian Ocean circulation, water mass, and biogeochemical properties. Section 3 focuses on the exports and imports that stem from the south of Australia. Section 4 features the exchanges that occur within the greater

This book has a companion website hosting complementary materials. Visit this URL to access it: https://www.elsevier.com/books-and-journals/book-companion/9780128226988.

FIG. 1 Schematic of the boundary current circulation around the Indian Ocean. Color contours are dynamic height (m² s⁻²) at the sea surface relative to 1975 m averaged between 2004 and 2015, estimated using the gridded Argo climatology data (Roemmich & Gilson, 2009). The solid teal arrows show the surface circulation in the New Guinea Coastal Current (NGCC), Mindanao Current (MC), Indonesian Throughflow (ITF), Leeuwin Current (LC), Tasman leakage (TL), Flinders Current (FC), South Equatorial Current (SEC), Eastern Madagascar Current (EMC), Agulhas Current (AC), Agulhas leakage (AL), Agulhas Return Current (ARC), and the SubAntarctic Front (SAF) of the Antarctic Circumpolar Current.



Agulhas system, and Section 5 details the Southern Ocean exchanges. Projected changes in all these interbasin connections in a warming world are briefly considered in Section 6, and conclusions are given in Section 7.

# 2 The Indonesian Throughflow

### 2.1 Introduction

The Indonesian seas provide the low-latitude pathway between the Pacific and Indian Oceans and play a critical role in regional climate, air—sea interaction, and the heat and freshwater budgets of the Indian Ocean. This unique choke point in the global ocean circulation allows for the transport of relatively warm low salinity tropical waters via multiple circuitous pathways collectively called the ITF (Fig. 2).

Strong easterly trade winds create high sea level in the tropical western Pacific, generating the Pacific–Indian interbasin pressure gradient that drives the ITF on annual and longer timescales (Wyrtki, 1987). Hence, any phenomena that influence

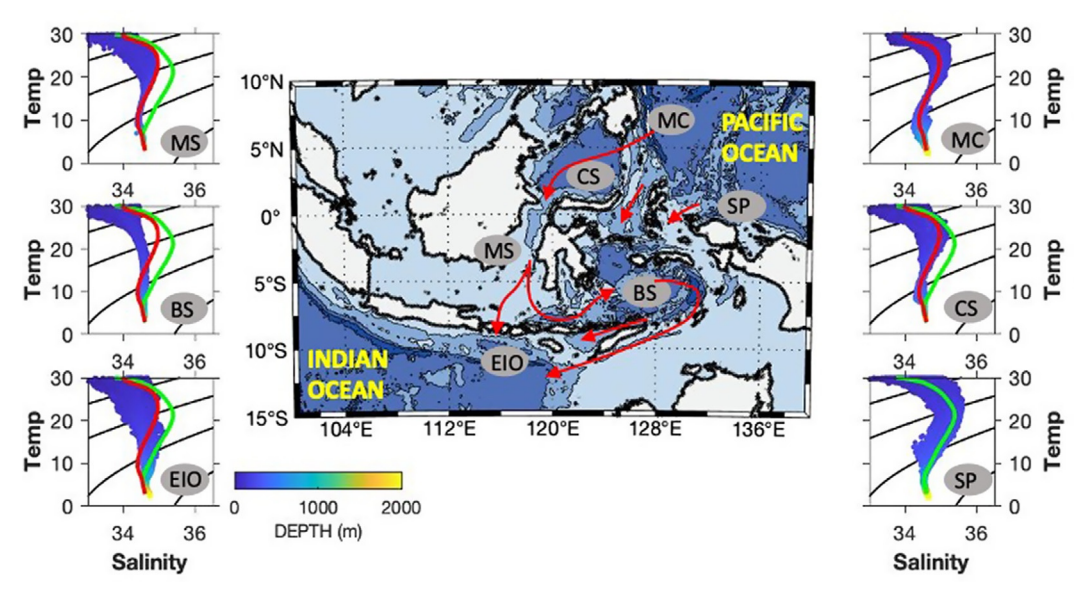


FIG. 2 Schematic of pathways of flow through the Indonesian seas. The side diagrams show the temperature (°C; y-axis) versus salinity (PSS-78; x-axis) diagrams color-coded by depth (m) in the inflow regions from the Mindanao Current (MC) and the South Pacific (SP) through the Celebes Sea (CS) into Makassar Strait (MS), then the Banda Sea (BS) and exiting into the Eastern Indian Ocean (EIO). In each panel, the *red* curve represents the isopycnal mean temperature and salinity in the MC of the North Pacific and the *green* curve represents the isopycnal mean temperature and salinity in the South Pacific. Note the erosion of both the salinity maxima in the thermocline layer and the salinity minimum at intermediate depth as the Pacific inflow waters traverse the regional Indonesia seas into the Indian Ocean. The temperature and salinity data are from the Argo climatology.

the strength or timing of this pressure gradient will, in turn, impact the ITF. One such phenomenon is the El Niño-Southern Oscillation (ENSO). During the La Niña phase, the Pacific trade winds are stronger and thereby increase the pressure gradient and enhance the ITF transport (e.g., Gordon et al., 2008, 2012). The opposite occurs during El Niño. ENSO can also affect temperature stratification, with a deepening of the thermocline during La Niña (Ffield et al., 2000; Susanto et al., 2012). These combined effects on the volume transport and temperature act to increase the ITF heat flux into the Indian Ocean during La Niña (Gruenburg & Gordon, 2018), especially during boreal summer months (Gordon et al., 2019). Similarly, on interdecadal timescales, the large-scale wind changes in the Pacific Walker Circulation associated with the Interdecadal Pacific Oscillation (IPO) can also impact the Indo-Pacific pressure gradient, changing the ITF transport and its subsequent influence on the Indian Ocean heat and freshwater (Hu & Sprintall, 2016; Ummenhofer et al., 2021). More details on the impact of the ITF on the Indian Ocean basin on decadal and longer time scales can be found in Tozuka et al. (2024).

On seasonal timescales, the annual reversal of winds associated with the large-scale East Asian Monsoon system causes a significant annual and semi-annual (during monsoon transitions) variation in the ITF transport with maxima typically occurring during the boreal summer season (Gordon et al., 2008, 2012; Sprintall et al., 2009; Susanto et al., 2012). Paleo coral records have shown that the strength of the monsoon can also change over time and this in turn modulates the ITF (Murty et al., 2017). This nonstationarity can challenge interpretation of longer-term trends related to both natural and anthropogenic forcing in the region (Ummenhofer et al., 2021).

# 2.2 Pathways through the Indonesian seas

The inflow of ITF waters is primarily drawn from the Mindanao (North Pacific) and Halmahera (South Pacific) Retroflections. Still, the ratio of the relatively fresher North Pacific to the saltier South Pacific contributions to the ITF and how this might change over time remains poorly understood. Most of the ITF is thought to originate from the North Pacific taking a western route through the Celebes Sea by way of Makassar Strait (Gordon & Fine, 1996). The North Pacific water is characterized by a salinity maximum in the upper thermocline layer and a salinity minimum in the lower thermocline intermediate layer (Fig. 2). Secondary portals of fresher North Pacific surface waters can also enter the Indonesian seas via the South China Sea to the Sulu Sea through the shallow Sibutu Passage as well as via the Karimata Strait between Sumatra and Kalimantan. Saltier lower thermocline and fresher intermediate South Pacific waters (Fig. 2) primarily enter via an eastern route through the Maluku and Halmahera Seas, as well as through density-driven overflows in the deep Lifamatola Passage that dominate the deeper layers of the Banda Sea (Van Aken et al., 1988). However, the various inflows via these northeastern passages remain inadequately observed and have poorly known pathways and transit times, which may vary over many timescales (Gordon et al., 2010).

As the North and South Pacific Ocean water masses make their way through into the internal Indonesian seas they undergo significant alteration. The salinity extrema of the Pacific source waters erode to create a unique Indonesian sea water mass with an intense thermocline but a more isohaline profile (Fig. 2). The water mass transformation seems to occur almost as soon as the Pacific waters enter the Indonesian seas (Koch-Larrouy et al., 2008; Sprintall et al., 2014). Processes causing the modification of the Pacific water masses include diapycnal mixing related to topography that induces strong internal tides (Koch-Larrouy et al., 2008, 2010, 2015), as well as contributions from enhanced air-sea heat and freshwater fluxes (Wijffels et al., 2008), and Ekman pumping induced by the monsoon winds (Gordon & Susanto, 2001).

The ITF water masses that are exported into the Indian Ocean are thus not the same water masses that entered the Pacific Ocean (Fig. 2). Flow into the Indian Ocean occurs primarily via the shallow Lombok Strait and the deeper exit channels of Ombai Strait and Timor Passage (Sprintall et al., 2009). However, because the vertical structure of the transport through each exit passage is quite different, each passage also admits distinct variants of the ITF water masses into the Indian Ocean. The transport profile is surface intensified in the wider Timor Passage but subsurface velocity maxima are evident in Ombai and Lombok Straits. A mean total volume transport of ∼15 Sv enters the Indian Ocean via these combined ITF exit channels with a mean transport weighted temperature of 17.9°C (Sprintall et al., 2009). However, the wide-ranging temporal variability of the wind and buoyancy forcings and the contrasting vertical profiles causes variability in the volume transport that can be as large as the mean, and this significantly impacts the subsequent amount of heat and freshwater transport that is partitioned through each channel into the Indian Ocean.

Local and remote wind forcing drives planetary waves that radiate and scatter into the Indonesian seas and affect the currents and water mass transformation. Pacific Ocean wind anomalies force low-frequency off-equatorial Rossby waves that interact with the western Pacific maritime boundary to excite coastally trapped waves that propagate through the Indonesian seas, along the northwest coast of Australia, subsequently generating Rossby waves that move offshore into the Indian Ocean (England & Huang, 2005; McClean et al., 2005; Wijffels & Meyers, 2004). In the Indian Ocean, equatorial wind anomalies on timescales ranging from intraseasonal to interannual spawn eastward propagating equatorial Kelvin waves. The Kelvin waves strongly impact the timing, location, and strength of the ITF exit flow (Drushka et al., 2010; Sprintall et al., 2009) and have been shown to radiate up into Makassar Strait and beyond (Hu et al., 2019; Napitu et al., 2019; Pujiana et al., 2013, 2019). Nonetheless, the impacts that planetary waves have on the water masses and residence times within the internal seas are not well known (Wijffels & Meyers, 2004).

#### 2.3 **Biogeochemistry within the Indonesian seas**

The Indonesian seas are an integral part of the "Coral Triangle," a vast network of abundant marine ecosystems that contains  $\sim 80\%$  of all the marine species in the Indo-Pacific region, making it a region of global significance for marine biodiversity (Roberts et al., 2002; Tun et al., 2004). The ITF is thought to be an important source of nutrients to the Indian Ocean (Ayers et al., 2014) although the North Pacific Mindanao Current that sources the ITF is not very rich in nutrients (Xie et al., 2019). Hence, the Indonesian seas themselves must act as a significant nutrient source. Strong mixing and upwelling within the Indonesian seas draw the nutrient-rich deeper waters upward to become available to primary producers (e.g., Broecker et al., 1986; Coatanoan et al., 1999; van Bennekom & Muchtar, 1988). River runoff into the Indonesian coastal regions provides large amounts of terrestrial organic matter that may also result in the delivery of nutrients (Asanuma et al., 2003; Hendiarti et al., 2004). The high percentage of diatoms in the euphotic zone within the Indonesian seas accumulates dissolved silica in the surface water, especially during the Southeast Monsoon in July-September (van Bennekom, 1988). The sedimentation of the diatom frustules and their subsequent dissolution then enriches the silica input throughout the water column (Talley & Sprintall, 2005). Silica concentrations are also observed to be relatively high in shallow waters, such as the Java Sea, which could be caused by a terrestrial silica supply via river runoff (Kartadikaraia et al., 2015).

Internal waves generated in response to the strong tidal flows within the internal Indonesian seas and in the vicinity of straits (Koch-Larrouy et al., 2007) induce changes in upper ocean stratification that impact chlorophyll blooms and primary productivity that are evident in remotely sensed imagery (Moore & Marra, 2002; Nugroho et al., 2018; Susanto et al., 2006; Xu et al., 2018). The seasonal reversal of monsoon winds appears to act like a "switch," turning on much higher primary production during the Southeast Monsoon and leaving an oligotrophic regime for the remainder of the year. The ENSO cycle acts in much the same way: the El Niño phase strengthens and lengthens the biological response to the Southeast Monsoon but has little apparent effect during the rest of the year (Moore et al., 2003).

Little attention has been given to the carbon budget within the Indonesian seas. The Indonesian seas are situated between appreciable CO<sub>2</sub> sink regions in the western Pacific ITF entrance and the Indian Ocean exit. However, overall the Indonesian seas appear to act as a  $CO_2$  source to the atmosphere with an air–sea flux of  $3.7 \pm 2.2 \, \text{mol m}^{-2}$  year<sup>-1</sup> (Kartadikaraia et al., 2015), consistent with that of other low-latitude coastal regions (Gruber, 2015). Nonetheless, significant regional differences are evident. The regional carbon cycle is influenced by the carbonate system, water mass characteristics, nutrients, organic matter, upwelling, river inflow, and atmospheric conditions. The shallow Karimata Strait and Java Sea release more CO<sub>2</sub> to the atmosphere compared to the deeper Flores and Banda Seas, while considerable CO<sub>2</sub> sinks have been observed in the northern Makassar Strait and the northern Banda Sea (Hamzah et al., 2020; Kartadikaraia et al., 2015). Physical mixing appears responsible for the carbon sink in the eastern seas. Somewhat surprisingly, temperature had only limited seasonal influence on the carbon cycle but becomes more significant during ENSO events (Kartadikaraia et al., 2015).

### The ITF influence on the properties and currents within the Indian Ocean

From the outflow passages, the signature of the Indonesian water mass is readily identifiable across nearly the entire Indian Ocean basin (e.g., Wyrtki, 1971) (Fig. 1). Observations show a separate low salinity surface core (Gordon et al., 1997) from a low salinity, high silicate intermediate depth core (Talley & Sprintall, 2005) within the South Equatorial Current between around 10° and 15°S. Somewhat paradoxically, because the ITF is relatively fresh compared to Indian Ocean water masses, the spreading of the ITF along isopycnal surfaces acts to cool and freshen the Indian Ocean (Song & Gordon, 2004; Talley & Sprintall, 2005).

Sharp biogeochemical fronts coincide with the hydrological fronts associated with the pathway of the ITF waters in the tropical Indian Ocean. The biogeochemical characteristics of the water masses that originate from the Indonesian seas have tracers that clearly separate the waters to the north and south in the Indian Ocean with distinct cores of elevated tritium (Fine, 1985) and high phosphate, nitrate, and silicate at mid-depth (Ayers et al., 2014; Coatanoan et al., 1999; Fieux et al., 1996) and a separate intermediate depth high silica core (Reid, 2003; Talley & Sprintall, 2005). The mid-depth signal occurs because the nutricline is elevated in the well-mixed Indonesian seas relative to that of the Indian Ocean subtropical gyre, and so appears as a larger effective nutrient flux within lighter density classes in the Indian Ocean (Ayers et al., 2014).

The nutrient enrichment by the ITF thermocline waters can support a substantial amount of new production and significantly impact the basin-wide biogeochemical cycles in the Indian Ocean (Ayers et al., 2014).

The ITF flow from the South Equatorial Current also contributes to the Agulhas Current system (Section 4). Le Bars et al. (2013) showed that ~10 Sv (two-thirds) of a modeled ITF transport arrives in the Agulhas Current, with 3 Sv of that exiting via the Agulhas leakage into the Atlantic while Durgadoo et al. (2017) found 6 Sv of ITF water contributes to the Agulhas leakage. These models suggest a 10- to 30-year timescale for the ITF water to reach the Agulhas region, and during the journey, the ITF waters are subject to significant cooling and salinification through air-sea interaction and mixing with the ambient saltier Indian Ocean water masses. Hence, upon entering the Atlantic Ocean, there is little resemblance of the water masses to the characteristic isohaline ITF profile that exited from the Indonesian seas into the southeast Indian Ocean. The ITF also feeds into the Leeuwin Current (Section 3.2.1), where changes in the ITF contribution can affect marine ecosystems along the West Australian coast (Feng et al., 2013).

In recent decades, the role of the ITF in interbasin heat exchange has been striking. During the period of global surface warming slowdown or "hiatus" in the early 21st century, numerous studies suggested that the excess atmospheric heat uptake within the Pacific Ocean was transferred westwards via the ITF resulting in an increase in upper ocean heat content within the Indian Ocean (Lee et al., 2015; Nieves et al., 2015; Zhang et al., 2018). This increase in upper ocean heat content contributed to a reduction in the meridional pressure gradient within the Indian basin acting to reduce the strength of the monsoonal winds (Vidya et al., 2020) and even influenced the Atlantic meridional overturning circulation (Hu & Fedorov, 2019, 2020). Further details on longer-term heat content related to decadal Indian Ocean variability are found in Tozuka et al. (2024).

# Southeastern boundary exchanges

#### 3.1 Introduction

A network of boundary currents along Australia's western and southern coastlines allows the exchange of waters between the Indian Ocean and the waters south of Australia. A schematic view (Fig. 3) illustrates the export from the Indian Ocean via the near-surface, poleward-flowing Leeuwin Current, and a recently identified deep eastern boundary current that both continue south of Australia (Tamsitt et al., 2019). Import into the Indian Ocean is accomplished by the Leeuwin Undercurrent at thermocline and intermediate depths and the Flinders Current and Tasman Outflow (or Tasman leakage) between the surface and intermediate depths. The general circulation within the Indian Ocean is discussed further in Phillips et al. (2024).

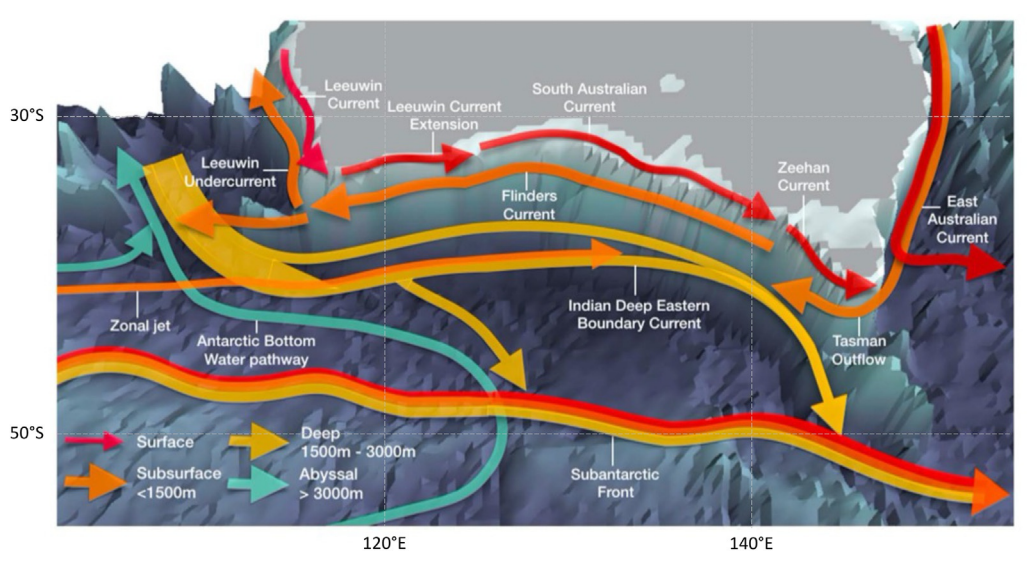


FIG. 3 Schematic of the circulation pathways of the southeastern Indian Ocean boundary exchanges south of Australia. Upper ocean current pathway on the continental shelf/slope is in red; subsurface (<1500 m) pathway in orange; deep (1500–3000 m) circulation in yellow; abyssal (>3000 m) circulation of Antarctic Bottom Water is shown in teal. The major currents and features of the region are labeled. (Figure from Tamsitt et al. (2019).)

#### 3.2 **Exports from the Indian Ocean**

# The Leeuwin Current

The Leeuwin Current is an eastern boundary current that uniquely flows poleward along the shelf break of Western Australia (Smith et al., 1991), unlike the equatorward flowing eastern boundary currents found elsewhere. It owes its existence to the strong meridional pressure gradient created by the presence of the warm, fresh ITF waters carried westward by the South Equatorial Current and denser subtropical waters to the south. This poleward decrease in pressure in the upper 200– 300 m drives eastward geostrophic currents from as far west as Madagascar toward the eastern boundary (Divakaran & Brassington, 2011; Domingues et al., 2007; Menezes et al., 2014; Palastanga et al., 2007; Phillips et al., 2024). As the bands of flow approach Australia, they veer southward because of the pressure gradient set up by the Australian landmass, inducing downwelling and a surface poleward current in opposition to the southerly winds along the coast (Furue et al., 2013; Godfrey & Ridgway, 1985; McCreary et al., 1986; Thompson, 1987).

The primary source waters to the Leeuwin Current are the near-surface eastward flow, the ITF, and a weaker source from the Holloway Current on the Australian Northwest Shelf. In the north, the Leeuwin Current waters are relatively fresh and warm due to their tropical origins (Andrews, 1977; Domingues et al., 2007; Legeckis & Cresswell, 1981; Phillips et al., 2005; Rochford, 1969; Woo & Pattiaratchi, 2008). As the Leeuwin Current flows poleward, the saltier surface waters of the subtropical South Indian Ocean and additional surface cooling together contribute to the Leeuwin Current densification (Domingues et al., 2006; Furue, 2019; Woo & Pattiaratchi, 2008).

The Leeuwin Current creates mixed barotropic and baroclinic instabilities that generate mesoscale eddies (Feng et al., 2005; Meuleners et al., 2007, 2008; Pearce & Griffiths, 1991). The eddies and energetic meandering drive the strongest eddy kinetic energy level found in any subtropical eastern boundary system (Fang & Morrow, 2003; Feng et al., 2005). The eddies thus play a key role in the momentum balance of the Leeuwin Current. In an eddy-permitting model, Domingues et al. (2006) found that 70% of the heat advected by the Leeuwin Current was exported by eddy heat fluxes to the ocean interior, facilitating a transfer of over  $40 \,\mathrm{W\,m^{-2}}$  of heat to the atmosphere in the southeast Indian Ocean. Anticyclonic eddies generated within the Leeuwin Current carry coastal water with elevated chlorophyll into the oligotrophic offshore waters, with enhanced productivity that can persist for months (Dufois et al., 2014; Feng et al., 2007; Moore et al., 2007; Phillips et al., 2021).

### The southern Australia current system

The Leeuwin Current pivots around the southwestern corner of Australia and continues to flow eastward in the Leeuwin Current Extension along the shelf break of the south coast of Australia (Duran et al., 2020b; Ridgway & Condie, 2004) (Fig. 3). It merges with a series of shelf-break currents that extend to the southern tip of Tasmania near 140°E. Starting from the North West Cape (21.8°S) off western Australia and extending to South East Cape, Tasmania (43.6°S), the combined Leeuwin Current and shelf-break currents represent the longest boundary circulation in the world (Middleton & Bye, 2007; Ridgway & Condie, 2004). The unique factors that contribute to this remarkably long boundary current are the ITF, which maintains the longshore pressure gradient off the west coast, and the uniquely broad zonal extent of the south coast of Australia (Ridgway & Condie, 2004). Monthly sea surface height anomalies (Fig. 4) show the gradual strengthening of the cross-shore pressure gradient, driving poleward flow along western Australia and continuing as eastward flow along southern Australia peaks in May–June (Ridgway & Condie, 2004).

The shelf-break currents are the surface expression of coupled surface and deep currents collectively known as the Southern Australia Current System (Duran et al., 2020b). The system contains the eastward shelf-break currents including the eastward Leeuwin Current Extension, the predominantly eastward South Australian Current, and the poleward Zeehan Current; the counter-flowing Flinders Current is an undercurrent to the shelf-break current along the shelf break but extends to the sea surface further offshore (Fig. 3). When the longshore surface current is weak, the shelf-break currents tend to be somewhat fragmentary (Oke et al., 2018) and sometimes even reverse (Duran et al., 2020b). For this reason, and also because of a lack of observations, the SBCs have not traditionally been viewed as a single current.

The forcing mechanisms of the flow on the western and southern Australian shelves are distinct. While the Leeuwin Current is driven by the longshore pressure gradient that overwhelms the local opposing winds (Section 3.2.1), the southern shelf-break currents are directly forced by the winds, with high coastal sea level established by onshore Ekman flow driven by the winter westerly wind. The seasonal timing of these two different forcing mechanisms means that the west coast pressure gradient, strongest in austral winter (Feng et al., 2003), delivers the Leeuwin Current to the south coast just as the winds reverse and are thus able to maintain the eastward passage of the shelf-break currents (Ridgway & Condie, 2004) (Fig. 4).

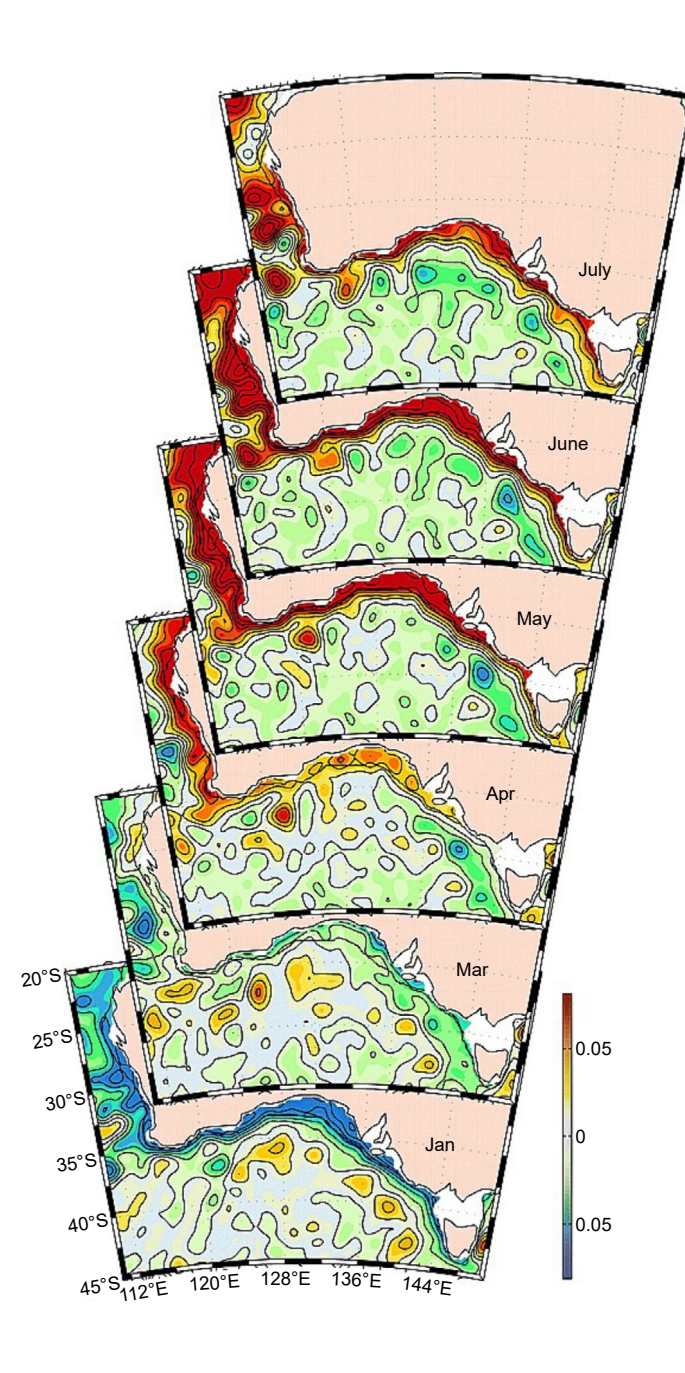


FIG. 4 Monthly composite maps (July through January) of the sea surface height along the western and southern Australian coastline illustrate the 5500km continuity of the southeastern boundary current of the Indian Ocean. The monthly sea surface height (m) maps are constructed from the merged remotely sensed altimetric data, month is indicated in each map, and contour interval is 0.02 m. (Figure from Ridgway and Condie (2004).)

The impact of the eastward shelf-break current on the ecology of the southern shelf region is extensive (Edyvane, 2000). The long distances traveled by biological organisms within the current system were in fact what led to the discovery of the 5500 km long boundary current (Maxwell & Cresswell, 1981; Saville-Kent, 1897). A range of observations provide evidence that demonstrates an "Indo-Pacific" character of waters in the Great Australian Bight (Maxwell & Cresswell, 1981). The presence of a subtropical eastward current flowing from Cape Leeuwin to western Bass Strait was surmised based on the distribution of dinoflagellates that are excellent indicators of water mass origins (Wood, 1954). Wood (1954) further suggested that the discovery of warm water turtles on the west coast of Tasmania confirmed the presence of the warm water current.

### A deep eastern boundary current

Poleward-flowing deep-water pathways exist along the eastern boundary of each Southern Hemisphere basin although their dynamics are not well understood (Faure & Speer, 2012; Schulze Chretien & Speer, 2018; Tamsitt et al., 2019; Van Sebille et al., 2012). The little-studied deep pathway in the eastern Indian Ocean was first suggested from oxygen, chlorofluorocarbon, and carbon sections (Hufford et al., 1997; Schodlok et al., 1997; Talley, 2013a, 2013b) and supported by some limited direct velocity measurements (McCartney & Donohue, 2007). The Deep Eastern Boundary Current spanning 1200–3000m depth along the southern boundary of Australia carries the low oxygen, high dissolved inorganic carbon signature characteristic of Indian Deep Water (Tamsitt et al., 2019), that is delivered to the upwelling regions of the Southern Ocean (Tamsitt et al., 2017, 2018, 2019).

The Deep Eastern Boundary Current is composed of two branches: eastward flow along the continental slope beneath the westward flowing Flinders Current and a second core of eastward flow offshore (Tamsitt et al., 2019) (Fig. 3). The offshore flow is part of a vertically coherent full-depth jet south of the Flinders Current (Duran et al., 2020b; Tamsitt et al., 2019). Models suggest the variability in the part of the Deep Eastern Boundary Current against the slope—the true boundary current—is strongly correlated to the variability in the Flinders Current above (Tamsitt et al., 2019). Part of the offshore Deep Eastern Boundary Current deviates southward between 120° and 130°E and appears to follow the abyssal path of the Antarctic Bottom Water inflow to the Indian Ocean. While the dynamics of the Deep Eastern Boundary Current are still unclear, eddy variability is thought to play a key role (Drake et al., 2018; Tamsitt et al., 2019).

#### 3.3 Imports to the Indian Ocean

#### 3.3.1 Leeuwin Undercurrent

Beneath and just offshore of the Leeuwin Current is the equatorward-flowing Leeuwin Undercurrent that extends from 200 to 900 m (Church et al., 1989; Furue et al., 2017; Smith et al., 1991; Thompson, 1984). The Leeuwin Undercurrent begins at Cape Leeuwin (34°S, 114°E) and is fed by a northward bend of a small fraction of the Flinders Current (Furue et al., 2017) (Fig. 3). Near 22°S, most of the Leeuwin Undercurrent leaves the continental slope and flows offshore (Duran, 2015; Furue et al., 2017; Zheng, 2018), apparently following the southern flank of the Exmouth Plateau although its vertical extent of 900m is much shallower than the Plateau.

The long-term average volume transport of the Leeuwin Undercurrent, based on the CARS 1/8-degree climatology (Ridgway et al., 2002), reveals a complex three-dimensional overturning circulation. The Leeuwin Undercurrent carries 0.2 Sv northward at its southern end and receives an additional inflow of 1.5 Sv from offshore between 32°S and 28°S that appears to be fed by a cyclonic recirculation of Flinders Current water around the Naturaliste Plateau. In addition to these imports, the Leeuwin Undercurrent also receives 3.5 Sv by a vertical exchange along isopycnals from the layer above that is supplied by shallow eastward flow into the Leeuwin Current from the Indian Ocean interior (Furue, 2019; Furue et al., 2017). At its northern end near 22°S, the Leeuwin Undercurrent loses 3.6 Sv to westward flow into the Indian Ocean interior and carries 1.7 Sv northward (Furue et al., 2017). No systematic seasonal variability of the Leeuwin Undercurrent was evident in the high-resolution CARS climatology nor in an eddy-permitting ocean model (Furue et al., 2017).

The upper part of the Leeuwin Undercurrent carries high salinity, low oxygen South Indian Central Water (Duran, 2015; Woo & Pattiaratchi, 2008) supplied by the downwelling along isopycnals from the layer above (Furue, 2019; Furue et al., 2017). The middle section of the Leeuwin Undercurrent carries cool, salty, high-oxygen Subantarctic Mode Water northward, centered near 400 m depth (Thompson, 1984; Woo & Pattiaratchi, 2008) and is also evident as a vertical minimum in potential vorticity (Duran, 2015). Antarctic Intermediate Water salinity minimum occupies the lower part of the Leeuwin Undercurrent in the depth range 600-900m, shoaling northward (Duran, 2015; Woo & Pattiaratchi, 2008). The Subantarctic Mode Water and Antarctic Intermediate Water water masses are most likely supplied to the Leeuwin Undercurrent by the 0.2 Sv at its southern end and the additional 1.7 Sv from the recirculation of the Flinders Current, based on the CARS climatology and an eddy-permitting ocean model (Furue et al., 2017). These Southern Ocean water mass signatures are still evident in the waters that outflow to the ocean interior at the northern end of the Leeuwin Undercurrent near 22°S (Duran, 2015; Zheng, 2018), forming a direct route from the Southern Ocean into the tropical Indian Ocean.

#### 3.3.2 Tasman leakage

A portion of the western boundary of East Australian Current that does not retroflect back into the Pacific Ocean finds its way into the Indian Ocean. This Tasman leakage (Ridgway & Dunn, 2003) is an important interocean contribution that, together with the ITF, builds the upper branch of the global thermohaline circulation passing through the Indian Ocean toward the Atlantic (Speich et al., 2002), thus connecting the subtropical gyres in all three oceans to form a "supergyre" (Speich et al., 2007).

High-resolution ocean models suggest that the Tasman leakage has a transport of about 4Sv with variability of about the same amplitude (Van Sebille et al., 2012, 2014). The main portion of Tasman leakage is found at intermediate depths that observational estimates report as  $3.8 \pm 1.3$  Sv (Rosell-Fieschi et al., 2013). Owing to a southward shift and increase in the Southern Hemisphere westerlies (Swart & Fyfe, 2012), the supergyre has spun up in recent decades (Cai, 2006; Duran et al., 2020a). However, it remains unclear and unconfirmed from oceanic hindcasts (i.e., ocean models forced by atmospheric reanalyzes) (Van Sebille et al., 2012, 2014) if the Tasman leakage has undergone a subsequent strengthening.

# 3.3.3 Flinders current

The Flinders Current, found between the surface and 2000 m depth, follows the southern Australian shelf break from the southern tip of Tasmania to Cape Leeuwin (Duran et al., 2020b; Middleton & Cirano, 2002) and continues westward into the Indian Ocean (Hufford et al., 1997; McCartney & Donohue, 2007). The Flinders Current is located beneath the shelfbreak currents along the continental slope but strengthens and shoals from east to west (Cresswell & Peterson, 1993; Duran et al., 2020b; Middleton & Bye, 2007).

Model experiments show the mechanism driving the Flinders Current is positive wind-stress curl in the South Australian Basin leading to a northward barotropic Sverdrup transport that is deflected westward along the southern Australia continental slope (Middleton & Cirano, 2002). Where the Flinders Current has a northward orientation along the coast (east of 132°E), the Sverdrup theory may fail because it is along an eastern boundary (McCreary, 1981; McCreary et al., 1991) and offshore propagation of Rossby waves should eliminate the current (Anderson & Gill, 1975). Recirculating flows in the South Australian Basin also supply the Flinders Current. In particular, the Flinders Current is the westward-flowing arm on the northern side of a large, quasi-stationary anticyclonic eddy off 120°E, known as the Albany High (Middleton & Bye, 2007) while the southern eastward-flowing arm coincides with a full depth eastward jet (McCartney & Donohue, 2007; Tamsitt et al., 2019) (see Section 3.2.3).

The Tasman leakage is a potential source of the Flinders Current (Feng et al., 2016; Middleton & Cirano, 2002; Rosell-Fieschi et al., 2013). However, an observational climatology and high-resolution ocean circulation model suggest that the Flinders Current receives no input from the Tasman leakage (Duran et al., 2020b). Rather, the entire Tasman leakage model transport of 11 Sv flows due west into the South Australian Basin. As the Flinders Current flows westward, its transport increases slightly to 1.9 Sv in the eastern Great Australian Bight, then increases more strongly once the shelf becomes zonal due to stronger onshore Ekman flows from the south. By the western end of the Bight, the transport is 7.8 Sv increasing to 12.3 Sv by Cape Leeuwin.

# The Agulhas leakage

### **Introduction to the greater Agulhas current system**

The Agulhas Current is the strongest western boundary current in the Southern Hemisphere and connects the Indian and Atlantic Oceans through the Agulhas leakage. This section describes the physical circulation within the Agulhas system, and we refer the interested reader to the reviews of Hood et al. (2017) and Phillips et al. (2021) for a discussion of biogeochemistry.

Although the dynamics of the Agulhas Current depend on the strength and interplay of the large-scale wind systems, it does not form a classical closure of interior Sverdrup dynamics (Beal et al., 2015; Biastoch et al., 2009b) like other western boundary currents. The Agulhas Current gathers additional transport through the thermohaline-driven global overturning circulation (Le Bars et al., 2013). Models typically simulate a nonlinear recirculation within the southwestern Indian Ocean subgyre (Biastoch et al., 2018; Loveday et al., 2014), although inverse models do not necessarily support its existence (Casal et al., 2009).

On a basin scale, the Agulhas Current is fed from the north by the ITF and by the Tasman leakage south of Australia (Fig. 5). Based on a Lagrangian analysis in a global eddy-rich model, Durgadoo et al. (2017) estimated that 10–11 Sv of the inflow from the Pacific arrives in the Agulhas Current through the Mozambique Channel and the East Madagascar Current. Other modeling and observational studies also support these sources (Biastoch & Krauss, 1999; De Ruijter et al., 2004; Halo et al., 2014; Schouten et al., 2002a). Smaller contributions come from the Persian Gulf and the Red Sea, the latter quite prominently shaping the high salinity below the thermocline and eroding the salinity minimum of the Antarctic Intermediate Water (Beal et al., 2006). The Indian Ocean significantly modifies the inflow water masses in their thermohaline properties, for example, cooling and salinifying the upper part of the ITF during its passage across the Indian Ocean (Durgadoo et al., 2017).

The Agulhas Current changes its character along its pathway toward the southern tip of Africa. The northern part, fully constituted south of 27°S, hugs the African shelf break in a v-shaped profile with surface velocities >1.5 m s<sup>-1</sup> in the apex (Lutjeharms, 2006). At 32°S, it reaches below 2000 m, transporting 78 Sv (Bryden et al., 2005, integrated over the upper

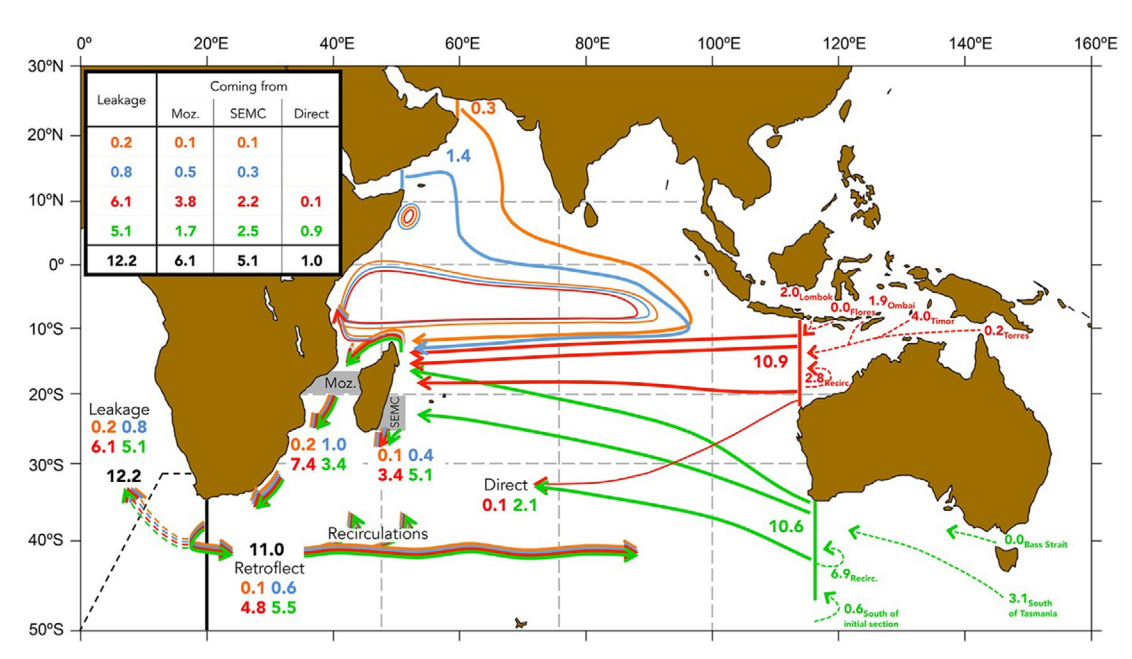


FIG. 5 Schematic of the major circulation pathways that cross longitude 20°E south of Africa. The transport (Sv) pathways are based on a Lagrangian analysis in a global eddy-rich model for a 100-year run. The 32.2 Sv total transport that crosses 20°E comes from the Persian Gulf (orange), the Red Sea (blue), the Indonesian Throughflow (ITF: red), and the Tasman leakage (TL: green), with a total transport of 12.2 Sv entering the Atlantic Ocean and 11 Sv in the Agulhas Retroflection. The table inset details the decomposition of the Agulhas leakage in Sv from the Mozambique Channel (Moz), the southeast Madagascar Current (SEMC), and directly from the interior Indian Ocean (direct). Sizes of the arrows vary only for clarity, dashed arrows itemize the upstream sources for the ITF and TL. (Figure from Durgadoo et al. (2017).)

2400 m). At 34°S, it has established a transport of  $84 \pm 24$  Sv (Beal & Elipot, 2016). South of  $\sim 34$ °S, where the shelf begins to widen, the upper part of the Agulhas Current can meander toward the coast. As a consequence, the Agulhas Current is highly variable and subject to nonlinear recirculation.

Along its pathway, the Agulhas Current is subject to occasional meanders, abruptly shifting the boundary current by more than 100km offshore (Fig. 6). These "Natal Pulses" occur 1.6 times per year on average (Elipot & Beal, 2015), although there are year-to-year variations (Yamagami et al., 2019). The Natal Pulses are a result of the mesoscale eddies arriving from within the Mozambique Channel and from the East Madagascar Current, interacting with the Agulhas Current through barotropic instability (Elipot & Beal, 2015; Tsugawa & Hasumi, 2010; Yamagami et al., 2019). Natal Pulses are a direct connection between the upstream sources and the variability south of Africa as described below (Schouten et al., 2002b).

At about 34°S, the African continent terminates, with the submerged Agulhas Bank forming a relatively shallow (<200 m) and wide (250 km) shelf. At 20°E, the Agulhas Current enters the Atlantic Ocean, but due to its inertia, flows for another five or more degrees of longitude into the South Atlantic. Because of the zero line of the wind stress curl positioned south of Africa, the Agulhas Current then retroflects, with the major portion returning into the Indian Ocean (Lutjeharms, 2006). This Agulhas Return Current loses water through recirculation in the subtropical gyre of the Indian Ocean, as it flows eastward and eventually completes the gyre circulation. The remainder of the Agulhas waters enter the Atlantic Ocean, quite distinctly as cyclonic and anticyclonic mesoscale features, the latter called Agulhas rings, but also in the form of a direct inflow. This Agulhas leakage connects the subtropical gyres to form the supergyre of the Southern Hemisphere (Speich et al., 2007).

Agulhas rings are among the largest and most long-lived mesoscale features in the world ocean, extending below 2000 m depth and featuring diameters of several 100 km (Chelton et al., 2011; Van Aken et al., 2003). Both the Agulhas Return Current and the ring shedding are subject to strong variability caused by internal dynamics and can be triggered by the Natal Pulses in the Agulhas Current (Elipot & Beal, 2015; Schouten et al., 2002b). Consequently, the amount of Agulhas leakage entering (and remaining in) the Atlantic Ocean is highly variable on a range of timescales (Biastoch et al., 2009b). Observational estimates of Agulhas leakage are challenged because of sparse data and the strong variability of the region. Using (at that time) all available surface drifters and surface floats, Richardson (2007) proposed a mean Agulhas leakage of 15 Sv for the upper 1000 m. A more recent update, including profiling floats, resulted in a leakage of  $21.3 \pm 4.7$  Sv

(Daher et al., 2020). Nonetheless, it remains unclear whether the updated higher amount is because the transport is estimated over the upper 2000 m or rather if it points to an increase of Agulhas leakage over time.

The Agulhas Current system also provides an exchange from west to east. Entering the Cape Basin as a sluggish flow from the north (Arhan et al., 2003), North Atlantic Deep Water finds its way around the Cape into the Indian Ocean. Part of the North Atlantic Deep Water is concentrated in a northward flow beneath the Agulhas Current. This Agulhas Undercurrent transports  $4.2 \pm 5.2$  Sv (Beal, 2009), albeit with high variability as a result of the interplay between the meandering Agulhas Current along the inshore that permits upwelling of deeper water masses (Biastoch et al., 2009a; Goschen et al., 2015; Leber et al., 2017).

# Temporal variability of the Agulhas current and Agulhas leakage

The transport of the Agulhas Current has short-term variations (Beal et al., 2015) possibly related to the intermittent Natal Pulses that introduce cyclonic circulations and steer the Agulhas Current offshore (Elipot & Beal, 2015). Owing to the high frequency and internal variability, the seasonal cycle of the Agulhas Current can be difficult to detect. Using a combination of observations from Argo hydrography, satellite altimetry, and mooring transports, McMonigal et al. (2018) found an annual cycle with a 22 Sv peak-to-peak amplitude, with a minimum in austral winter and a maximum in austral summer. Seasonal changes in the Agulhas Current transport are related to the timescale of Rossby waves communicating the wind change from the southern Indian Ocean into the Agulhas regime (Hutchinson et al., 2018). In contrast to the volume transport, the temperature transport of the Agulhas Current and hence the amount of warm water brought from the equatorial Indian Ocean to the southern tip of Africa does not indicate a clear seasonal cycle (McMonigal et al., 2020), although it varies in response to the presence of meanders (Fig. 6). Over longer timescales, Beal and Elipot (2016) showed that enhanced eddy activity and associated meandering have caused the Agulhas Current to broaden instead of strengthen since the early 1990s.

In addition to the external drivers of variability, the nonlinearity in the system creates a significant level of internal variability. Biastoch et al. (2009b) demonstrated that both the Agulhas Current transport and the Agulhas leakage display the same level of interannual variability, independent of whether the atmospheric forcing shows year-to-year variability or not. Since the interannual variability is in large part dominated by internal variability, the influence of large-scale climate

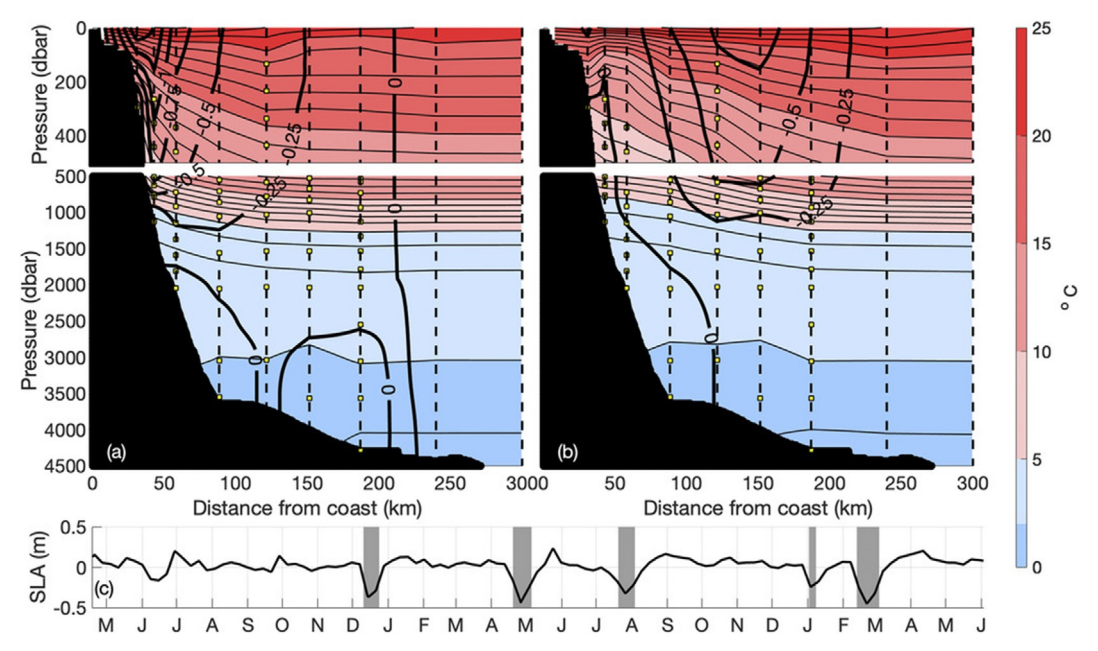


FIG. 6 Temperature and velocity structure are affected by meandering of the Agulhas Current. Mean temperature (°C; colors and thin contours) and mean cross-track velocity (m s<sup>-1</sup>; thick contours) estimated from April 2016 to June 2018 moored observations in the Agulhas Current during (a) nonmeandering and (b) meandering periods. The temperature contour interval is 1°C and the velocity contour interval is 0.25 m s<sup>-1</sup>. (c) Time series of sea level anomaly (SLA, m) at 33.6°S, 28°E in the Agulhas Current is used to define meanders when SLA < 0.2 m (gray shading). (Figure from McMonigal et al. (2020).)

modes on the Agulhas Current system is hard to detect. Paris et al. (2018) found that the warm Indian Ocean during El Niño becomes evident in the Agulhas leakage region as a subsurface signal 2 years after the event, communicated by baroclinic Rossby waves. Using a coupled climate model, Putrasahan et al. (2016) also linked sea surface temperature variability in the Agulhas Current to El Niño events. While ENSO explains  $\sim 11.5\%$  of the variance of the Agulhas Current transport, the interannual Southern Annular Mode does not show a significant correlation (Elipot & Beal, 2018).

Oceanic hindcasts demonstrate a strengthening of the Southern Hemisphere westerlies that has increased the Agulhas leakage by more than 1.2 Sv per decade, or 30% from the 1960s to the 2000s (Biastoch et al., 2009b; Durgadoo et al., 2013; Schwarzkopf et al., 2019). An observational index for the Agulhas leakage, based on the SST difference between the Cape Basin and the Agulhas Return Current (Biastoch et al., 2015), suggests a similar transport increase from the 1960s with a leveling off occurring in the 1990s. This confirms that Agulhas leakage is not only subject to strong interannual variability but also suggests decadal variability and a general increasing trend.

#### 4.3 Impact of the Agulhas leakage on the Atlantic Ocean

Agulhas leakage forms an important part of the global overturning circulation and injects salt into the Atlantic Ocean, potentially stabilizing a declining Atlantic Meridional Overturning Circulation (AMOC) (Beal et al., 2011). Agulhas leakage impacts the Atlantic Ocean in two ways: through a planetary wave response and through an advection of water masses.

Systematically isolating the mesoscale dynamics in the Agulhas Current region using a nested model approach, Biastoch et al. (2008) demonstrated that decadal anomalies of 1-2Sv in the Agulhas leakage stem from the Agulhas dynamics and are rapidly communicated toward the North Atlantic. The signals find their way to the Northern Hemisphere after only a few years, through an interplay between westward propagating Agulhas rings and/or baroclinic Rossby waves crossing the South Atlantic that induce fast propagating topographic shelf waves along the American continental margin. The waves themselves do not transport any water masses but have the potential to lift and lower the density interfaces far away from the southern tip of Africa and hence induce additional variability within the AMOC.

More important than the wave effect is the transfer of water masses from the Indian to the Atlantic Ocean. Since the Indian is warmer and more saline than the Atlantic at the same latitude on either side of the African continent, the Agulhas leakage provides a fan of warm and saline waters into the Atlantic. The estimated Agulhas Leakage fluxes are 0.2 PW of heat and  $8 \times 10^{13}$  kg yr<sup>-1</sup> of salt (Biastoch et al., 2015; Gunn et al., 2020; McMonigal et al., 2020). The leakage is most visible at depth (see Fig. 2 in Biastoch et al., 2008) but is also evident in SST (Biastoch et al., 2015). Part of the Agulhas leakage recirculates within the subtropical gyre of the South Atlantic, whereby more than half finds its way toward the equator, primarily transported by the North Brazil Undercurrent, and then into the North Atlantic (Rühs et al., 2013, 2019).

Agulhas leakage warms and salinifies the Atlantic Ocean (Biastoch et al., 2015; Lübbecke et al., 2015). In a series of sensitivity experiments, Lee et al. (2011) demonstrated that the increase in North Atlantic heat content since the mid-20th century can be explained by the injection of warmer water from the Agulhas Current system. Changing wind systems may also affect the flow from the Pacific toward the Atlantic, eventually compensating for part of the Agulhas leakage through fresher and colder water masses (Cessi & Jones, 2017; Rühs et al., 2019). In addition, both contributions (particularly their upper portions) are significantly modified through air-sea exchange on their way toward the North Atlantic (Rousselet et al., 2020; Rühs et al., 2019).

#### 5 **Southern Ocean water mass exchanges**

The Indian Ocean also exchanges water, heat, and other properties across its large southern border with the Southern Ocean. Exchanges between these two oceans are often described by the movement of water masses across a zonal transect from southern Africa to western Australia along 32°S (Fig. 7). Multiple full-depth hydrographic sampling of this transect has been conducted since 1987, repeated roughly every 7-10 years. Estimates across 32°S of the meridional overturning circulation within the Indian Ocean are quite varied, ranging from ~10 Sv (Bryden & Beal, 2001; Ganachaud et al., 2000) to ~27 Sv (Toole & Warren, 1993). Here we focus on the water masses exchanged across the 32°S Southern Ocean boundary. A more detailed discussion of the pathways of the Indian Ocean meridional overturning circulation is found in Phillips et al. (2024).

In the upper water column at 32°S, Subantarctic Mode Water flows equatorward and is distinguishable by its relatively high oxygen in a thick thermostad layer in the upper 300–500 m (Fig. 7). Subantarctic Mode Water forms east of the Kerguelen Plateau between the Subantarctic and Subtropical Fronts in the northern Antarctic Circumpolar Current from unusually deep winter mixed layers (Sallée et al., 2006). These waters then flow northward and westward, subducting into

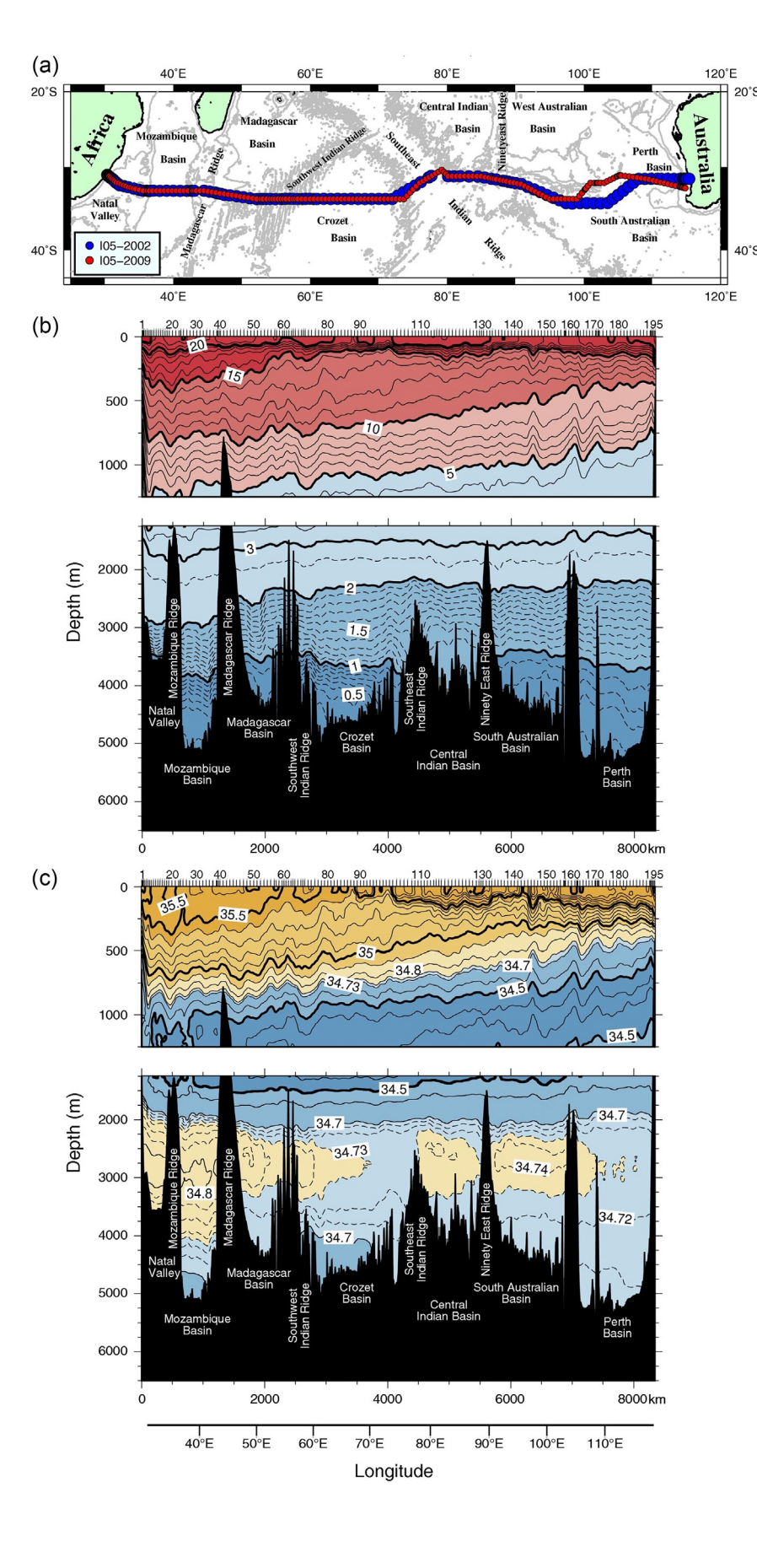


FIG. 7 Water mass properties across the 32°S Southern Ocean boundary of the Indian Ocean. (a) Station map of repeat hydrographic section along 32°S in 2002 and 2009. Vertical sections along the transect of (b) potential temperature (°C) and (c) practical salinity. Blackshading is the sea floor bathymetry with key features marked. (Figure from Hernandez-Guerra and Talley (2016).)

the subtropical Indian Ocean (Herraiz-Borreguero & Rintoul, 2011) and ventilating the subthermocline (Hanawa & Talley, 2001) throughout the Indian Ocean. The subsurface oxygen maximum associated with Subantarctic Mode Water is observed as far north as the poleward side of the South Equatorial Current and even further north along the western boundary within the Somali Current (Talley et al., 2011). The Antarctic Intermediate Water exists as a low salinity layer beneath the Subantarctic Mode Water, also flowing equatorward across the 32°S boundary. While Subantarctic Mode Water is strongest in the eastern part of the basin, Antarctic Intermediate Water is most prominent in the western half (Fine, 1993). Both Subantarctic Mode Water and Antarctic Intermediate Water return southward across 32°S within the Agulhas Current.

No deep waters are formed within the Indian Ocean basin itself; therefore, all abyssal water masses enter from the Southern Ocean. As in all ocean basins, the deep pathways are largely constrained by the seafloor topography. Deep water masses including Circumpolar Deep Water, North Atlantic Deep Water, and Antarctic Bottom Water flow northward in deep western boundary currents along Madagascar and African coasts in the western Indian, and along the Southeast Indian and Ninety-East Ridges in the eastern Indian Ocean. Antarctic Bottom Water is the primary deep water within the Indian Basin, with the volume of North Atlantic Deep Water contributing around 10%–20% (Johnson, 2008). Since the 1990s, abyssal water masses within the Indian Ocean have experienced warming, although this signal seems mainly constrained to the deep basins east of the Ninety-East Ridge and weakens to the north (Purkey, 2010). Collectively, the deep waters are upwelled within the Indian Ocean and then return south to exit the basin at shallower depths as part of the return flow within the meridional overturning circulation.

# **Predicted changes to Interbasin boundary current connections**

Climate models project robust changes in the global ocean circulation in response to greenhouse gas and other anthropogenic forcing, and the current systems that participate in the interbasin connections with the Indian Ocean are no exception. Nonetheless, there can be challenges to the confidence in the simulated predictions since these boundary currents are often poorly represented in coupled climate models partly because of bias in the forcing terms (particularly the winds), but also because the models' coarse horizontal resolutions (often 1–2 degree) are unable to realistically resolve the narrow jets and eddy variability that are characteristic of the boundary flows. Various approaches are used to somewhat alleviate these concerns such as the application of ensembles constructed from multiple climate models that enable some assessment of the statistical uncertainty. More recently, global eddy-resolving ocean model projections have been constructed and in addition, many studies have embedded regionally downscaled higher-resolution models under the premise that these eddy-resolving models have greater fidelity to the observations and provide sharper details in boundary currents. However, downscaled ocean-only models can also omit the important physics associated with air-sea interaction in boundary current regions. With these model limitations and caveats in mind, here we highlight some of the recent projections of change in the current streams that feed into and out of the Indian Ocean basin. Additional information on future projections within the Indian Ocean can be found in Roxy et al. (2024).

A growing consensus of climate models projects a decrease in the ITF mass and heat transport in a warming world by as much as 20%-30% of the modern-day transport estimates under the RCP8.5 scenario that assumes an increase of greenhouse gases reaches ~1370 ppm CO<sub>2</sub>-equivalent concentrations by 2100 (Feng et al., 2017; Hu et al., 2015; Ma et al., 2020; Sen Gupta et al., 2016; Stellema et al., 2019; Sun et al., 2012). Nonetheless, there remains some debate as to the ultimate drivers of the ITF weakening. Future trade winds in the equatorial Pacific Ocean are projected to decrease, driving a weaker Mindanao Current that is the dominant contributor to the ITF (Hu et al., 2015; Sen Gupta et al., 2012), and hence one might expect this to subsequently produce a slowdown in the ITF. However, various studies have questioned whether the decrease in the Mindanao Current is sufficient to fully explain the ITF change (Hu et al., 2015) and indeed there appears little relationship in the Climate Model Intercomparison Project (CMIP) models between the variability in the Mindanao Current and that of the ITF (Sen Gupta et al., 2016). One alternative hypothesis suggested for the ITF transport weakening is a projected reduction in the upwelling and circulation of the deep waters entering the Pacific from the Southern Ocean that ultimately upwell to exit via the ITF (Feng et al., 2017; Sen Gupta et al., 2016). Another hypothesis suggests that the weakened ITF on centennial time scales is closely tied to a projected weakening of the AMOC (Cheng et al., 2013; Weijer et al., 2020) that initiates a transient response that propagates into the Indian Ocean via planetary waves, acting to reduce the Indo-Pacific pressure gradient responsible for the ITF (Sun & Thompson, 2020). The relative importance of local and remotely driven wind and buoyancy processes on the projected variability of the ITF within CMIP simulations requires further analysis.

Both CMIP (Stellema et al., 2019) and ocean downscaled models (Sun et al., 2012) also project a weakening of the Leeuwin Current, on average by about 5%–10% by the end of the 21st century under the RCP8.5 high emissions scenario, albeit with large intermodel differences. This transport reduction has been primarily attributed to reduced onshore flow in response to the weakening of the longshore pressure gradient that sets up the Leeuwin Current. Using regional downscaled models, Sun et al. (2012) suggested this was consistent with the projected weakening of the ITF. However, more recent CMIP5 multimodel analyses show little correspondence between the projected variability in the ITF and the Leeuwin Current (Stellema et al., 2019). Hence, it remains unclear what drives the longshore change in sea surface height on these longer time scales. Significant decreases are also projected in the Leeuwin Undercurrent due to a reduction in the westward outflow from the Flinders Current system south of Australia (Stellema et al., 2019).

Multiple climate models forecast a robust weakening in the East Madagascar Current and through the Mozambique Channel with a corresponding weakening of transport (11%–23%) into the Agulhas Current under increased greenhouse gas emission RCP8.5 scenarios (Stellema et al., 2019). The weakened Agulhas transport reduces the southward heat transport out of the Indian Ocean, which together with increased air-sea heat flux input, is projected to amplify the already significant Indian Ocean warming trend (Cheng et al., 2017; Ma et al., 2020; Roxy et al., 2014). CMIP5 analysis suggests the reduction in the greater Agulhas system appears to be partially related to the reduced ITF and partially related to an overall slow-down of the Indian Ocean meridional overturning circulation manifested as more sluggish equatorward deep flow and reduced upwelling that ultimately acts to reduce the basin-wide upper-ocean outflow (Stellema et al., 2019). Future coupled climate models that adequately simulate mesoscale processes will be critical for determining the key mechanisms responsible for driving projected oceanic changes in energetic regions such as the Agulhas Current system.

In contrast to the weakening Agulhas Current, the Agulhas leakage south of Africa into the Atlantic Ocean is consistently projected to strengthen with climate change (Biastoch & Böning, 2013; Stellema et al., 2019). In a warming world, the Southern Ocean westerlies are anticipated to intensify and shift poleward and consequently there is a southward expansion in the subtropical supergyre (Cai, 2006; Sen Gupta et al., 2009) and subsequent increase in the Agulhas leakage (Biastoch & Böning, 2013). As a result, the enhanced contribution of saltier Indian Ocean water causes a net gain in density within the Atlantic Ocean that may potentially counteract some of the projected slow-down in the AMOC due to greenhouse warming (Weijer & van Sebille, 2014).

# **Conclusions**

This chapter has highlighted the oceanic interbasin exchanges of mass and other properties into and out of the Indian Ocean via a series of complex pathways.

The transport of Pacific waters into the Indian Ocean via the ITF affects the salinity, temperature, and nutrient budgets of the Indian Ocean and serves as a pathway for the propagation of oceanic waves. The ITF is influenced by a wide array of regional climate forcing on intraseasonal timescales, the Indian Ocean Dipole and ENSO on interannual timescales, and the IPO on decadal timescales and potentially anthropogenic activity on longer timescales. Nonetheless, a paucity of observations in the Indonesian seas, particularly of marine biogeochemistry, means that there remains a relatively poor understanding of the gating of the flow and properties through the maritime continent and their influence on the Indian Ocean basin.

The Leeuwin Current system provides an efficient route for Indian Ocean surface and deep waters to be exported poleward and for intermediate waters from the Southern Ocean to penetrate into the tropical Indian Ocean. This route is due to the unique presence of the ITF exiting into the southeast Indian Ocean and does not exist in any other basin. The recent availability of Argo hydrographic profiles invigorated the discovery of new current pathways, such as westward outflow from the Leeuwin Undercurrent (Furue, 2019; Furue et al., 2017; Zheng, 2018) and the Deep Eastern Boundary Current (Tamsitt et al., 2019) south of Australia.

Surface transport from the Pacific Ocean via both the ITF and the Tasman leakage crosses the Indian Ocean to join the Agulhas system south of Africa, albeit undergoing strong water mass changes along the way. The Agulhas Current is the strongest of the Southern Hemisphere's western boundary currents and is subject to vigorous dynamics through wind and internal variability. Export into the Atlantic Ocean via the Agulhas leakage is highly nonlinear and exhibits strong decadal variability and long-term trends.

Along the southern border of the Indian Ocean, the inflow of mode and intermediate waters from the Southern Ocean acts to ventilate the basin. The deep limb of the meridional overturning circulation is characterized by the topographically constrained inflow of deep waters that then upwell and return via the Agulhas western boundary current system and the southward flow of Indian Deep Water. Changes in the property characteristics and pathways of these waters can affect the circulation, ocean heat content, and sea level rise.

Projected changes in the oceanic teleconnection pathways due to a warming climate are expected to alter the Indian Ocean circulation. In contrast to the modern world, the Indian Ocean projections of inflow from the ITF and outflow via the Leeuwin Current and the Agulhas Current system appear to show relatively little co-variability on climate time

scales. However, there remains much uncertainty given that these narrow and eddying boundary currents are poorly simulated in coarse resolution climate models. Nonetheless, future changes in the Indian Ocean boundary currents will have important implications for marine ecosystems and connectivity (Barange et al., 2014; Bopp et al., 2013; Funk et al., 2008) and hence are of significant consequence for the Indian Ocean rim countries that rely on marine resources for their sustenance and economic well-being.

#### **Educational resources** 8

Additional general references that describe sampling and data collection in the boundary currents of the Indian Ocean can be found in:

Wyrtki, K. (1971). Oceanographic Atlas of the International Indian Ocean Expedition. National Science Foundation, Washington, D.C., 531 pp.

Beal, L.M., Vialard, J., Roxy, M.K., and lead authors (2019). Executive Summary. IndOOS-2: A roadmap to sustained observations of the Indian Ocean for 2020–2030. CLIVAR-4/2019, GOOS-237, 204 pp. https://doi.org/10.36071/clivar. rp.4.2019.

Beal, L.M., et al. (2020). A roadmap to IndOOS-2: Better observations of the rapidly-warming Indian Ocean, Bulletin of the American Meteorological Society. https://doi.org/10.1175/BAMS-D-19-0209.1.

Hermes, J.C., et al. (2019). A sustained ocean observing system in the Indian Ocean for climate related scientific knowledge and societal needs, Frontiers of Marine Sciences. https://doi.org/10.3389/fmars.2019.00355.

# Acknowledgments

JS acknowledges funding to support her effort by the National Science Foundation under Grant Number OCE-1851316. HEP acknowledges support from the Australian Government Department of the Environment and Energy National Environmental Science Programme, the Australian Government Department of the Environment and Energy National Environmental Science Programme, the Australian Government Department of the Environment and Energy National Environmental Science Programme, the Australian Government Department of the Environment and Energy National Environmental Science Programme, the Australian Government Department of the Environment Department of the Environment Department of the Environment and Energy National Environmental Science Programme, the Australian Government Department of the Environment Department D tralian Government Antarctic Science Collaboration Initiative (ASCI000002), and the ARC Centre of Excellence in Climate Extremes.

## **Author contributions**

JS led the overall writing, editing, and organization of the manuscript. JS wrote Sections 1 and 6; LKG and JS wrote Section 2; HEP and AB wrote Section 3; AB wrote Section 4; HEP and LKG wrote Section 5; all authors wrote Section 7. All authors contributed comments and feedback on the overall structure of the chapter and contributed to revisions.

# References

- Anderson, D. L., & Gill, A. (1975). Spin-up of a stratified ocean, with applications to upwelling. Deep Sea Research and Oceanographic Abstracts, 22(9), 583-596. https://doi.org/10.1016/0011-7471(75)90046-7.
- Andrews, J. C. (1977). Eddy structure and the West Australian current. Deep Sea Research, 24(12), 1133-1148. https://doi.org/10.1016/0146-6291(77) 90517-3.
- Arhan, M., Mercier, H., & Park, Y.-H. (2003). On the deep water circulation of the eastern South Atlantic Ocean. Deep Sea Research Part 1: Oceanographic Research Papers, 50, 889-916. https://doi.org/10.1016/S0967-0637(03)00072-4.
- Asanuma, I., Matsumoto, K., Okano, H., Kawano, T., Hendiarti, N., & Sachoemar, S. I. (2003). Spatial distribution of phytoplankton along the Sunda Islands: The monsoon anomaly in 1998. Journal of Geophysical Research, Oceans. https://doi.org/10.1029/1999jc000139.
- Ayers, J. M., Strutton, P. G., Coles, V. J., Hood, R. R., & Matear, R. J. (2014). Indonesian throughflow nutrient fluxes and their potential impact on Indian Ocean productivity. Geophysical Research Letters, 41(14), 5060-5067. https://doi.org/10.1002/2014GL060593.
- Barange, M., Merino, G., Blanchard, J., et al. (2014). Impacts of climate change on marine ecosystem production in societies dependent on fisheries. Nature Climate Change, 4, 211–216. https://doi.org/10.1038/nclimate2119.
- Beal, L. M. (2009). A time series of Agulhas undercurrent transport. Journal of Physical Oceanography, 39, 2436-2450. https://doi.org/10.1175/ 2009JPO4195.1.
- Beal, L. M., Chereskin, T. K., Lenn, Y. D., & Elipot, S. (2006). The sources and mixing characteristics of the Agulhas current. Journal of Physical Oceanography, 36, 2060-2074. https://doi.org/10.1175/JPO2964.1.
- Beal, L. M., De Ruijter, W. P. M., Biastoch, A., Zahn, R., & members of S. W. G. (2011). On the role of the Agulhas system in ocean circulation and climate. Nature, 472(7344), 429-436. https://doi.org/10.1038/nature09983.
- Beal, L. M., & Elipot, S. (2016). Broadening not strengthening of the Agulhas current since the early 1990s. Nature. https://doi.org/10.1038/nature19853. Beal, L. M., Elipot, S., Houk, A., & Leber, G. M. (2015). Capturing the transport variability of a western boundary jet: Results from the Agulhas current time-series experiment (ACT). Journal of Physical Oceanography, 45(5), 1302-1324. https://doi.org/10.1175/JPO-D-14-0119.1.

- Biastoch, A., Beal, L. M., Lutjeharms, J. R. E., & Casal, T. G. D. (2009a). Variability and coherence of the Agulhas undercurrent in a high-resolution ocean general circulation model. Journal of Physical Oceanography, 39(10), 2417-2435. https://doi.org/10.1175/2009JPO4184.1.
- Biastoch, A., & Böning, C. W. (2013). Anthropogenic impact on Agulhas leakage. Geophysical Research Letters, 40, 1138–1143. https://doi.org/10.1002/ grl.50243.
- Biastoch, A., Böning, C. W., & Lutjeharms, J. R. E. (2008). Agulhas leakage dynamics affects decadal variability in Atlantic overturning circulation. Nature, 456(7221), 489–492. https://doi.org/10.1038/nature07426.
- Biastoch, A., Böning, C. W., Schwarzkopf, F. U., & Lutjeharms, J. R. E. (2009b). Increase in Agulhas leakage due to poleward shift of southern hemisphere westerlies. Nature, 462(7272), 495-498. https://doi.org/10.1038/nature08519.
- Biastoch, A., Durgadoo, J. V., Morrison, A. K., Van Sebille, E., Weijer, W., & Griffies, S. M. (2015). Atlantic multi-decadal oscillation covaries with Agulhas leakage. Nature Communications, 6, 10082. https://doi.org/10.1038/ncomms10082.
- Biastoch, A., & Krauss, W. (1999). The role of mesoscale eddies in the source regions of the Agulhas current. Journal of Physical Oceanography, 29(9), 2303-2317. https://doi.org/10.1175/1520-0485(1999)029<2303:TROMEI>2.0.CO;2.
- Biastoch, A., Sein, D., Durgadoo, J. V., & Wang, Q. (2018). Simulating the Agulhas system in global ocean models—Nesting vs. multi-resolution unstructured meshes. Ocean Modelling, 121, 117-131. https://doi.org/10.1016/j.ocemod.2017.12.002.
- Bopp, L., Resplandy, L., Orr, J. C., Doney, S. C., Dunne, J. P., Gehlen, M., Halloran, P., Heinze, C., Ilyina, T., Séférian, R., Tjiputra, J., & Vichi, M. (2013). Multiple stressors of ocean ecosystems in the 21st century: Projections with CMIP5 models. Biogeosciences, 10, 6225–6245. https://doi.org/10.5194/ bg-10-6225-2013.
- Broecker, W. S., Patzert, W. C., Toggweiler, J. R., & Stuiver, M. (1986). Hydrography, chemistry, and radioisotopes in the Southeast Asian basins. Journal of Geophysical Research. https://doi.org/10.1029/jc091ic12p14345.
- Bryden, H. L., & Beal, L. M. (2001). Role of the Agulhas current in Indian Ocean circulation and associated heat and freshwater fluxes. Deep Sea Research, Part I, 48, 1821-1845.
- Bryden, H. L., Beal, L. M., & Duncan, L. M. (2005). Structure and transport of the Agulhas current and its temporal variability. *Journal of Oceanography*, 61, 479-492.
- Cai, W. (2006). Antarctic ozone depletion causes an intensification of the Southern Ocean super-gyre circulation. Geophysical Research Letters, 33, L03712. https://doi.org/10.1029/2005GL024911.
- Caputi, N., Fletcher, W. J., Pearce, A., & Chubb, C. F. (1996). Effect of the Leeuwin current on the recruitment of fish and invertebrates along the Western Australian coast. Marine and Freshwater Research. https://doi.org/10.1071/MF9960147.
- Casal, T. G. D., Beal, L. M., Lumpkin, R., & Johns, W. E. (2009). Structure and downstream evolution of the Agulhas current system during a quasi-synoptic survey in February-march 2003. Journal of Geophysical Research, 114, C03001. https://doi.org/10.1029/2008JC004954.
- Cessi, P., & Jones, C. S. (2017). Warm-route versus cold-route interbasin exchange in the meridional overturning circulation. Journal of Physical Oceanography, 47(8), 1981-1997. https://doi.org/10.1175/JPO-D-16-0249.1.
- Chelton, D. B., Schlax, M. G., & Samelson, R. M. (2011). Global observations of nonlinear mesoscale eddies. *Progress in Oceanography*, 91(2), 167–216. https://doi.org/10.1016/j.pocean.2011.01.002.
- Cheng, W., Chiang, J. C. H., & Zhang, D. (2013). Atlantic meridional overturning circulation (AMOC) in CMIP5 models: RCP and historical simulations. Journal of Climate, 26, 7187-7197.
- Cheng, L., Trenberth, K. E., Fasullo, J., Boyer, T., Abraham, J., & Zhu, J. (2017). Improved estimates of ocean heat content from 1960 to 2015. Science Advances, 3(3), 1-10. https://doi.org/10.1126/sciadv.1601545.
- Church, J. A., Cresswell, G. R., & Godfrey, J. S. (1989). The Leeuwin current. In S. J. Neshyba, C. N. K. Mooers, R. L. Smith, & R. T. Barber (Eds.), Vol. 34. Poleward flows along eastern ocean boundaries, coastal and estuarine studies (formerly lecture notes on coastal and estuarine studies) (pp. 230–254). New York: Springer. https://doi.org/10.1007/978-1-4613-8963-7\_16.
- Coatanoan, C., Metzl, N., Fieux, M., & Coste, B. (1999). Seasonal water mass distribution in the Indonesian throughflow entering the Indian Ocean. Journal of Geophysical Research: Oceans, 104(C9), 20801-20826. https://doi.org/10.1029/1999jc900129.
- Cresswell, G. R., & Peterson, J. L. (1993). The Leeuwin current south of Western Australia. Marine and Freshwater Research. https://doi.org/10.1071/ MF9930285.
- Daher, H., Beal, L. M., & Schwarzkopf, F. U. (2020). A new improved estimation of Agulhas leakage using observations and simulations of Lagrangian floats and drifters. Journal of Geophysical Research, Oceans. https://doi.org/10.1029/2019JC015753.
- De Ruijter, W. P. M., Aken, H. M., Beier, E. J., Lutjeharms, J. R. E., Matano, R. P., & Schouten, M. W. (2004). Eddies and dipoles around South Madagascar: Formation, pathways and large-scale impact. Deep Sea Research, Part I, 51(3), 383-400.
- Divakaran, P., & Brassington, G. B. (2011). Arterial Ocean circulation of the Southeast Indian Ocean. Geophysical Research Letters, 38, L01802. https:// doi.org/10.1029/2010GL045574.
- Domingues, C. M., Maltrud, M. E., Wijffels, S. E., Church, J. A., & Tomczak, M. (2007). Simulated Lagrangian pathways between the Leeuwin current system and the upper-ocean circulation of the Southeast Indian Ocean. Deep Sea Research, Part II, 54, 797-817. https://doi.org/10.1016/j. dsr2.2006.10.003.
- Domingues, C. M., Wijffels, S. E., Maltrud, M. E., Church, J. A., & Tomczak, M. (2006). Role of eddies in cooling the Leeuwin current. Geophysical Research Letters, 33.
- Drake, H., Morrison, A. K., Griffies, S. M., Sarmiento, J. L., Weijer, W., & Gray, A. R. (2018). Lagrangian timescales of Southern Ocean upwelling in a hierarchy of model resolutions. Geophysical Research Letters, 45, 891-898. https://doi.org/10.1002/2017GL076045.

- Drushka, K., Sprintall, J., & Gille, S. T. (2010). Vertical structure of Kelvin waves in the Indonesian Throughflow exit passages. Journal of Physical Oceanography, 40, 1965-1987.
- Dufois, F., Hardman-Mountford, N. J., Greenwood, J., Richardson, A. J., Feng, M., Herbette, S., & Matear, R. (2014). Impact of eddies on surface chlorophyll in the South Indian Ocean. Journal of Geophysical Research, Oceans, 119, 8061-8077. https://doi.org/10.1002/2014JC010164.
- Duran, E. R. (2015). An investigation of the Leeuwin undercurrent source waters and pathways. (Honours thesis). University of Tasmania.
- Duran, E. R., England, M. H., & Spence, P. (2020a). Surface ocean warming around Australia driven by interannual variability and long-term trends in Southern Hemisphere westerlies. Geophysical Research Letters, 47, e2019GL086605. https://doi.org/10.1029/2019GL086605.
- Duran, E. R., Phillips, H. E., Furue, R., Spence, P., & Bindoff, N. L. (2020b). Southern Australia current system based on a gridded hydrography and a highresolution model. Progress in Oceanography. https://doi.org/10.1016/j.pocean.2019.102254.
- Durgadoo, J. V., Loveday, B. R., Reason, C. J. C., Penven, P., & Biastoch, A. (2013). Agulhas leakage predominantly responds to the southern hemisphere westerlies. Journal of Physical Oceanography, 43(10).
- Durgadoo, J. V., Rühs, S., Biastoch, A., & Böning, C. W. B. (2017). Indian Ocean sources of Agulhas leakage. Journal of Geophysical Research: Oceans, 122(4), 3481-3499. https://doi.org/10.1002/2016JC012676.
- Edyvane, K. (2000). The great Australian bight. In C. R. C. Sheppard (Ed.), Vol. II. Seas at the millennium: An environmental evaluation (pp. 673-690). New York: Pergamon.
- Elipot, S., & Beal, L. M. (2015). Characteristics, energetics, and origins of Agulhas current meanders and their limited influence on ring shedding. Journal of Physical Oceanography, 150626133140004. https://doi.org/10.1175/JPO-D-14-0254.1.
- Elipot, S., & Beal, L. M. (2018). Observed Agulhas current sensitivity to interannual and long-term trend atmospheric forcings. Journal of Climate, 31(8), 3077-3098. https://doi.org/10.1175/JCLI-D-17-0597.1.
- England, M., & Huang, F. (2005). On the interannual variability of the Indonesian Throughflow and its linkage with ENSO. Journal of Climate, 18(9), 1435-1444. https://doi.org/10.1175/JCLI3322.1.
- Fang, F., & Morrow, R. (2003). Evolution, movement and decay of warm-core Leeuwin current eddies. Deep Sea Research, Part II, 50(12-13), 2245-2261. https://doi.org/10.1016/S0967-0645(03)00055-9.
- Faure, V., & Speer, K. (2012). Deep circulation in the eastern South Pacific Ocean. Journal of Marine Research, 70(5), 748-778.
- Feng, M., Majewski, L. J., Fandry, C. B., & Waite, A. M. (2007). Characteristics of two counter-rotating eddies in the Leeuwin current system off the Western Australian coast. Deep Sea Research, Part II, 54(8-10), 961-980. https://doi.org/10.1016/j.dsr2.2006.11.022.
- Feng, M., McPhaden, M. J., Xie, S., & Hafner, J. (2013). La Niña forces unprecedented Leeuwin current warming in 2011. Scientific Reports, 3.
- Feng, M., Meyers, G., Pearce, A., & Wijffels, S. (2003). Annual and interannual variations of the Leeuwin current at 32 degrees S. Journal of Geophysical Research, Oceans, 108(C11).
- Feng, M., Wijffels, S., Godfrey, S., & Meyers, G. (2005). Do eddies play a role in the momentum balance of the Leeuwin current? Journal of Physical Oceanography, 35, 964-975.
- Feng, M., Zhang, X., Oke, P., Monselesan, D., Chamberlain, M., Matear, R., & Schiller, A. (2016). Invigorating ocean boundary current systems around Australia during 1979–2014: As simulated in a near-global eddy-resolving ocean model. Journal of Geophysical Research, Oceans, 121, 3395–3408.
- Feng, M., Zhang, X., Sloyan, B., & Chamberlain, M. (2017). Contribution of the deep ocean to the centennial changes of the Indonesian Throughflow. Geophysical Research Letters, 44(6), 2859–2867. https://doi.org/10.1002/2017GL072577.
- Ffield, A., Vranes, K., Gordon, A. L., Susanto, R. D., & Garzoli, S. L. (2000). Temperature variability within the Makassar Strait. Geophysical Research Letters, 27, 237-240.
- Fieux, M., Andrié, C., Charriaud, E., Ilahude, A. G., Metzl, N., Molcard, R., & Swallow, J. C. (1996). Hydrological and chlorofluoromethane measurements of the Indonesian throughflow entering the Indian Ocean. Journal of Geophysical Research, C: Oceans. https://doi.org/10.1029/96JC00207.
- Fine, R. A. (1985). Direct evidence using tritium data for throughflow from the Pacific into the Indian Ocean. Nature. https://doi.org/10.1038/315478a0. Fine, R. A. (1993). Circulation of Antarctic intermediate water in the South Indian Ocean. Deep Sea Research, Part 1, 40, 2021–2042.
- Funk, C., Dettinger, M. D., Michaelsen, J. C., Verdin, J. P., Brown, M. E., Barlow, M., & Hoell, A. (2008). Warming of the Indian Ocean threatens eastern and southern African food security but could be mitigated by agricultural development. Proceedings of the National Academy of Sciences, 105(32), 11081-11086.
- Furue, R. (2019). The three-dimensional structure of the Leeuwin current system in density coordinates in an eddy-resolving OGCM. Ocean Modelling, 138, 36-50. https://doi.org/10.1016/j.ocemod.2019.03.001.
- Furue, R., Guerreiro, K., Phillips, H. E., McCreary, J. P., Jr., & Bindoff, N. L. (2017). On the Leeuwin current system and its linkage to zonal flows in the South Indian Ocean as inferred from a gridded hydrography. Journal of Physical Oceanography, 47, 583-602.
- Furue, R., McCreary, J. P., Benthuysen, J., Phillips, H., & Bindoff, N. (2013). Dynamics of the Leeuwin current: Part 1. Coastal flows in an inviscid, variable-density, layer model. Dynamics of Atmospheres and Oceans, 63, 24-59.
- Ganachaud, A., Wunsch, C., Marotzke, J., & Toole, J. (2000). Meridional overturning and large-scale circulation of the Indian Ocean. Journal of Geophysical Research, Oceans. https://doi.org/10.1029/2000JC900122.
- Godfrey, J. S., & Ridgway, K. R. (1985). The large-scale environment of the poleward-flowing Leeuwin current, Western Australia: Longshore steric height gradients, wind stresses and geostrophic flow. Journal of Physical Oceanography. https://doi.org/10.1175/1520-0485(1985)015<0481: tlseot>2.0.co;2.
- Gordon, A. L. (1986). Interocean exchange of thermocline water. Journal of Geophysical Research. https://doi.org/10.1029/jc091ic04p05037.
- Gordon, A. L., & Fine, R. (1996). Pathways of water between the Pacific and Indian oceans in the Indonesian seas. Nature, 379, 146-149.

- Gordon, A. L., Huber, B. A., Metzger, J., Susanto, R. D., Hulbert, H. E., & Adi, T. R. (2012). South China Sea throughflow impact on the Indonesian throughflow. Geophysical Research Letters, 39, LI1602.
- Gordon, A. L., Ma, S., Olson, D. B., Hacker, P., Ffield, A., Talley, L. D., Wilson, D., & Baringer, M. (1997). Advection and diffusion of Indonesian throughflow water within the Indian Ocean south equatorial current. Geophysical Research Letters, 24, 2573–2576.
- Gordon, A. L., Napitu, A., Huber, B. A., Gruenburg, L. K., Pujiana, K., Agustiadi, T., Kuswardani, A., Mbay, N., & Setiawan, A. (2019). Makassar Strait throughflow seasonal and interannual variability: An overview. Journal of Geophysical Research, Oceans, 124. https://doi.org/10.1029/ 2018IC014502
- Gordon, A. L., Sprintall, J., Van Aken, H. M., Susanto, D., Wijffels, S., Molcard, R., Ffield, A., Pranowo, W., & Wirasantosa, S. (2010). The Indonesian Throughflow during 2004-2006 as observed by the INSTANT program in modeling and observing the Indonesian Throughflow. In A. L. Gordon, & V. M. Kamenkovich (Eds.), Vol. 50. Dynamics of atmosphere and oceans (pp. 115-128). https://doi.org/10.1016/j.dynatmoce.2009.12.002.
- Gordon, A. L., & Susanto, R. D. (2001). Banda Sea surface-layer divergence. Ocean Dynamics, 52(1), 2–10.
- Gordon, A. L., Susanto, R. D., Ffield, A., Huber, B. A., Pranowo, W., & Wirasantosa, S. (2008). Makassar Strait throughflow, 2004 to 2006. Geophysical Research Letters, 35, L24605.
- Goschen, W. S., Bornman, T. G., Deyzel, S. H. P., & Schumann, E. H. (2015). Coastal upwelling on the far eastern Agulhas Bank associated with large meanders in the Agulhas current. Continental Shelf Research, 101, 34-46. https://doi.org/10.1016/j.csr.2015.04.004.
- Gruber, N. (2015). Ocean biogeochemistry: Carbon at the coastal interface. Nature, https://doi.org/10.1038/nature14082.
- Gruenburg, L. K., & Gordon, A. L. (2018). Variability in Makassar Strait heat flux and its effect on the eastern tropical Indian Ocean. Oceanography, 31(2), 80-87.
- Gunn, K. L., Beal, L. M., Elipot, S., McMonigal, K., & Houk, A. (2020). Mixing of subtropical, central, and intermediate waters driven by shifting and pulsing of the Agulhas current. Journal of Physical Oceanography, 50, 3545-3560. https://doi.org/10.1175/JPO-D-20-0093.1.
- Halo, I., Penven, P., Backeberg, B., Ansorge, I., Shillington, F., & Roman, R. (2014). Mesoscale eddy variability in the southern extension of the East Madagascar Current: Seasonal cycle, energy conversion terms, and eddy mean properties. Journal of Geophysical Research: Oceans, 119(10), 7324-7356. https://doi.org/10.1002/2014JC009820.
- Hamzah, F., Agustiadi, T., Susanto, R. D., Wei, Z., Guo, L., Cao, Z., & Dai, M. (2020). Dynamics of the carbonate system in the western Indonesian seas during the southeast monsoon. Journal of Geophysical Research: Oceans, 125(1), 1–18. https://doi.org/10.1029/2018JC014912.
- Hanawa, K., & Talley, L. (2001). In G. Siedler, & J. Church (Eds.), International Geophysics Series. Ocean circulation and climate, chapter mode waters (pp. 373-386). New York: Academic.
- Hendiarti, N., Siegel, H., & Ohde, T. (2004). Investigation of different coastal processes in Indonesian waters using SeaWiFS data. Deep Sea Research Part II: Topical Studies in Oceanography. https://doi.org/10.1016/j.dsr2.2003.10.003.
- Hernandez-Guerra, A., & Talley, L. D. (2016). Meridional overturning transports at 30°S in the Indian and Pacific oceans in 2002-2003 and 2009. Progress in Oceanography, 146, 89-120. https://doi.org/10.1016/j.pocean.2016.06.005.
- Herraiz-Borreguero, L., & Rintoul, S. R. (2011). Subantarctic mode water: Distribution and circulation. Ocean Dynamics, 61, 103-126.
- Hood, R. R., Beckley, L. E., & Wiggert, J. D. (2017). Biogeochemical and ecological impacts of boundary currents in the Indian Ocean. Progress in Oceanography, 156, 290-325.
- Hu, S., & Fedorov, A. V. (2019). Indian Ocean warming can strengthen the Atlantic meridional overturning circulation. Nature Climate Change, 9, 747-751. https://doi.org/10.1038/s41558-019-0566-x.
- Hu, S., & Fedorov, A. V. (2020). Indian Ocean warming as a driver of the North Atlantic warming hole. Nature Communications, 11, 4785. https://doi.org/ 10.1038/s41467-020-18522-5.
- Hu, S., & Sprintall, J. (2016). Interannual variability of the Indonesian Throughflow: The salinity effect. Journal of Geophysical Research, 121, 2596-2615. https://doi.org/10.1002/2015JC011495.
- Hu, X., Sprintall, J., Yuan, D., Tranchant, B., Gaspar, P., Koch-Larrouy, A., Reffray, G., Li, X., Wang, Z., Li, Y., Nugroho, D., Corvianawatie, C., & Surinati, D. (2019). Interannual variability of the Sulawesi Sea circulation forced by indo-Pacific planetary waves. Journal of Geophysical Research, Oceans. https://doi.org/10.1029/2018JC014356.
- Hu, D., Wu, L., Cai, W., Gupta, A. S., Ganachaud, A., Qiu, B., et al. (2015). Pacific western boundary currents and their roles in climate. Nature, 522 (7556). https://doi.org/10.1038/nature14504.
- Hufford, G. E., McCartney, M. S., & Donohue, K. A. (1997). Northern boundary currents and adjacent recirculations off southwestern Australia. Geophysical Research Letters, 24(22), 2797-2800.
- Hutchinson, K., Beal, L. M., Penven, P., Ansorge, I., & Hermes, J. (2018). Seasonal phasing of Agulhas current transport tied to a baroclinic adjustment of near-field winds. Journal of Geophysical Research: Oceans, 123(10), 7067–7083. https://doi.org/10.1029/2018JC014319.
- Johnson, G. C. (2008). Quantifying Antarctic bottom water and North Atlantic deep water volumes. Journal of Geophysical Research, Oceans. https://doi. org/10.1029/2007JC004477.
- Kartadikaraia, A. R., Watanabe, A., Nadaoka, K., Adi, N. S., Prayitno, H. B., Soemorumekso, S., Muchtar, M., Triyulianti, I., Setiawan, A., Suratno, S., & Khasanah, E. N. (2015). CO2 sink/source characteristics in the tropical Indonesian seas. Journal of Geophysical Research: Oceans, 7842-7856. https://doi.org/10.1002/2015JC010925.Received.
- Koch-Larrouy, A., Atmadipoera, A., van Beek, P., Madec, G., Aucan, J., Lyard, F., Grelet, J., & Souhaut, M. (2015). Estimates of tidal mixing in the Indonesian archipelago from multidisciplinary INDOMIX in-situ data. Deep Sea Research, Part I, 106, 136-153. DSR1-D-14-00245R1.
- Koch-Larrouy, A., Lengaigne, M., Terray, P., Madec, G., & Masson, S. (2010). Tidal mixing in the Indonesian seas and its effect on the tropical climate system. Climate Dynamics, 34, 891-904.

- Koch-Larrouy, A., Madec, G., Bouruet-Aubertot, P., Gerkema, T., Bessières, L., & Molcard, R. (2007). On the transformation of Pacific water into Indonesian Throughflow water by internal tidal mixing. Geophysical Research Letters. https://doi.org/10.1029/2006GL028405.
- Koch-Larrouy, A., Madec, G., Iudicone, D., Molcard, R., & Atmadipoera, A. (2008). Physical processes contributing in the water mass transformation of the Indonesian ThroughFlow. Ocean Dynamics, 58, 275–288.
- Le Bars, D., Dijkstra, H. A., & De Ruijter, W. P. M. (2013). Impact of the Indonesian Throughflow on Agulhas leakage. Ocean Science, 9(5), 773-785. https://doi.org/10.5194/os-9-773-2013.
- Leber, G. M., Beal, L. M., & Elipot, S. (2017). Wind and current forcing combine to drive strong upwelling in the Agulhas current. Journal of Physical Oceanography, 47(1), 123–134. https://doi.org/10.1175/JPO-D-16-0079.1.
- Lee, S.-K., Park, W., Baringer, M. O., Gordon, A. L., Huber, B., & Liu, Y. (2015). Pacific origin of the abrupt increase in Indian Ocean heat content during the warming hiatus. Nature Geoscience, 8, 445-449. https://doi.org/10.1038/ngeo2438.
- Lee, S.-K., Park, W., van Sebille, E., Baringer, M. O., Wang, C., Enfield, D. B., et al. (2011). What caused the significant increase in Atlantic Ocean heat content since the mid-20th century? Geophysical Research Letters, 38(17), L17607. https://doi.org/10.1029/2011GL048856.
- Legeckis, R., & Cresswell, G. (1981). Satellite observations of sea-surface temperature fronts off the coast of western and southern Australia. Deep Sea Research, Part I, 28, 297-306. https://doi.org/10.1016/0198-0149(81)90069-8.
- Loveday, B. R., Durgadoo, J. V., Reason, C. J. C., Biastoch, A., & Penven, P. (2014). Decoupling the Agulhas current and Agulhas leakage. Journal of Physical Oceanography, 44, 1776–1797. https://doi.org/10.1175/JPO-D-13-093.1.
- Lübbecke, J. F., Durgadoo, J. V., & Biastoch, A. (2015). Contribution of increased agulhas leakage to tropical Atlantic warming. Journal of Climate, 28(24). https://doi.org/10.1175/JCLI-D-15-0258.1.
- Lutjeharms, J. R. E. (2006). The Agulhas. Current. https://doi.org/10.1007/3-540-37212-1.
- Ma, J., Feng, M., Lan, J., & Hu, D. (2020). Projected future changes of meridional heat transport and heat balance of the Indian Ocean. Geophysical Research Letters, 47(4), e2019GL086803. https://doi.org/10.1029/2019GL086803.
- Maxwell, J. G. H., & Cresswell, G. R. (1981). Dispersal of tropical marine fauna to the great Australian bight by the Leeuwin current. Australian Journal of Marine and Freshwater Research, 32, 493-500.
- McCartney, M. S., & Donohue, K. A. (2007). A deep cyclonic gyre in the Australian-Antarctic Basin. Progress in Oceanography, 75(4), 675–750.
- McClean, J. L., Ivanova, D. P., & Sprintall, J. (2005). Remote origins of interannual variability in the Indonesian Throughflow region from data and a global parallel ocean program simulation. Journal of Geophysical Research, 110, C10013. https://doi.org/10.1029/2004JC002477.
- McCreary, J. P. (1981). A linear stratified ocean model of the equatorial undercurrent. Philosophical Transactions of the Royal Society A Mathematical Physical and Engineering Sciences, 298(1444), 603-635. https://doi.org/10.1098/rsta.1981.0002.
- McCreary, J. P., Fukamachi, Y., & Kundu, P. K. (1991). A numerical investigation of jets and eddies near an eastern ocean boundary. Journal of Geophysical Research, Oceans, 96(C2), 2515-2534. https://doi.org/10.1029/90JC02195.
- McCreary, J. P., Shetye, S. R., & Kundu, P. K. (1986). Thermohaline forcing of eastern boundary currents: With application to the circulation off the west coast of Australia. Journal of Marine Research, 44, 71-92. https://doi.org/10.1357/002224086788460184.
- McMonigal, K., Beal, L. M., Elipot, S., Gunn, K. L., Hermes, J., Morris, T., & Houk, A. (2020). The impact of meanders, deepening and broadening, and seasonality on Agulhas current temperature variability. Journal of Physical Oceanography. https://doi.org/10.1175/jpo-d-20-0018.1.
- McMonigal, K., Beal, L. M., & Willis, J. K. (2018). The seasonal cycle of the South Indian Ocean subtropical gyre circulation as revealed by Argo and satellite data. Geophysical Research Letters, 45(17), 9034–9041. https://doi.org/10.1029/2018GL078420.
- Menezes, V. V., Phillips, H. E., Schiller, A., Bindoff, N. L., Domingues, C. M., & Vianna, M. L. (2014). South Indian countercurrent and associated fronts. Journal of Geophysical Research, Oceans, 119, 6763–6791. https://doi.org/10.1002/2014JC010076.
- Meuleners, M. J., Ivey, G. N., & Pattiaratchi, C. B. (2008). A numerical study of the eddying characteristics of the Leeuwin current system. Deep Sea Research, Part I, 55(3), 261-276. https://doi.org/10.1016/j.dsr.2007.12.004.
- Meuleners, M. J., Pattiaratchi, C. B., & Ivey, G. N. (2007). Numerical modelling of the mean flow characteristics of the Leeuwin current system. Deep Sea Research, Part II, 54(8-10), 837-858. https://doi.org/10.1016/j.dsr2.2007.02.003.
- Middleton, J. F., & Bye, J. A. T. (2007). A review of the shelf-slope circulation along Australia's southern shelves: Cape Leeuwin to Portland. Progress in Oceanography, 75(1), 1–41. https://doi.org/10.1016/j.pocean.2007.07.001.
- Middleton, J. F., & Cirano, M. (2002). A northern boundary current along Australia's southern shelves: The Flinders current. Journal of Geophysical Research, Oceans. https://doi.org/10.1029/2000jc000701.
- Moore, T. S., & Marra, J. (2002). Satellite observations of bloom events in the strait of Ombai: Relationships to monsoons and ENSO. Geochemistry, Geophysics, Geosystems. https://doi.org/10.1029/2001gc000174.
- Moore, T. S., Marra, J., & Alkatiri, A. (2003). Response of the Banda Sea to the southeast monsoon. Marine Ecology Progress Series. https://doi.org/ 10.3354/meps261041.
- Moore, T. S., Matear, R. J., Marra, J., & Clementson, L. (2007). Phytoplankton variability off the Western Australian coast: Mesoscale eddies and their role in cross-shelf exchange. Deep Sea Research Part II: Topical Studies in Oceanography. https://doi.org/10.1016/j.dsr2.2007.02.006.
- Murty, S. A., Goodkin, N. F., Halide, H., Natawidjaja, D., Suwargadi, B., Suprihasnto, I., ... Gordon, A. L. (2017). Climatic influences on southern Makassar Strait salinity over the past century. Geophysical Research Letters, 44, 11967–11975. https://doi.org/10.1002/2017GL075504.
- Napitu, A. M., Pujiana, K., & Gordon, A. L. (2019). The madden-Julian Oscillation's impact on the Makassar Strait surface layer transport. Journal of Geophysical Research. https://doi.org/10.1029/2018JC014729.
- Nieves, V., Willis, J. K., & Patzert, W. C. (2015). Recent hiatus caused by decadal shift in Indo-Pacific heating. Science, 349, 532-535. https://doi.org/ 10.1126/science.aaa4521.

- Nugroho, D., Koch-Larrouy, A., Gaspar, P., Lyard, F., Reffray, G., & Tranchant, B. (2018). Modelling explicit tides in the Indonesian seas: An important process for surface sea water properties. Marine Pollution Bulletin. https://doi.org/10.1016/j.marpolbul.2017.06.033.
- Oke, P. R., Griffin, D. A., Rykova, T., & de Oliveira, H. B. (2018). Ocean circulation in the great Australian bight in an eddy-resolving ocean reanalysis: The eddy field, seasonal and interannual variability. Deep Sea Research, Part II, 157–158, 11–26. https://doi.org/10.1016/j. dsr2.2018.09.012.
- Palastanga, V., van Leeuwen, P. J., Schouten, M. W., & de Ruijter, W. P. M. (2007). Flow structure and variability in the subtropical Indian Ocean: Instability of the South Indian Ocean countercurrent. Journal of Geophysical Research, 112, C01001. https://doi.org/10.1029/2005JC003395.
- Paris, M. L., Subrahmanyam, B., Trott, C. B., & Murty, V. S. N. (2018). Influence of ENSO events on the Agulhas leakage region. Remote Sensing in Earth Systems Sciences, 1(3-4), 79-88. https://doi.org/10.1007/s41976-018-0007-z.
- Pearce, A. F., & Griffiths, R. W. (1991). The mesoscale structure of the Leeuwin current: A comparison of laboratory model and satellite images. *Journal of* Geophysical Research, 96, 16730–16757. https://doi.org/10.1029/91JC01712.
- Phillips, H. E., Menezes, V. V., Nagura, M., McPhaden, M. J., Vinayachandran, P. N., & Beal, L. M. (2024). Chapter 8: Indian Ocean circulation. In C. C. Ummenhofer, & R. R. Hood (Eds.), The Indian Ocean and its role in the global climate system (pp. 169-203). Amsterdam: Elsevier. https://doi.org/10. 1016/B978-0-12-822698-8.00012-3.
- Phillips, H. E., Tandon, A., Furue, R., Hood, R., Ummenhofer, C., Benthuysen, J., Menezes, V., Hu, S., Webber, B., Sanchez-Franks, A., Cherian, D., Shroyer, E., Feng, M., Wijeskera, H., Chatterjee, A., Yu, L., Hermes, J., Murtugudde, R., Tozuka, T., ... Wiggert, J. (2021). Progress in understanding of Indian Ocean circulation, variability, air-sea exchange and impacts on biogeochemistry. Ocean Science, 17, 1677–1751. https://doi.org/10.5194/os-
- Phillips, H. E., Wijffels, S. E., & Feng, M. (2005). Interannual variability in the freshwater content of the Indonesian-Australian Basin. Geophysical Research Letters, 32, L03603. https://doi.org/10.1029/2004GL021755.
- Pujiana, K., Gordon, A. L., & Sprintall, J. (2013). Intraseasonal Kelvin waves in Makassar Strait. Journal of Geophysical Research, 118, 2023–2034.
- Pujiana, K., McPhaden, M. J., Gordon, A. L., & Napitu, A. M. (2019). Unprecedented response of Indonesian throughflow to anomalous Indo-Pacific climatic forcing in 2016. Journal of Geophysical Research. https://doi.org/10.1029/2018JC014574.
- Purkey, S. G., & Johnson, G. C. (2010). Warming of global abyssal and deep Southern Ocean waters between the 1990s and 2000s: Contributions to global heat and sea level rise budgets. Journal of Climate, 23, 6336-6351.
- Putrasahan, D., Kirtman, B. P., & Beal, L. M. (2016). Modulation of SST interannual variability in the Agulhas leakage region associated with ENSO. Journal of Climate, 29(19), 7089-7102. https://doi.org/10.1175/JCLI-D-15-0172.1.
- Reid, J. L. (2003). On the total geostrophic circulation of the Indian Ocean: Flow patterns, tracers, and transports. Progress in Oceanography. https://doi. org/10.1016/S0079-6611(02)00141-6.
- Richardson, P. L. (2007). Agulhas leakage into the Atlantic estimated with subsurface floats and surface drifters. Deep-Sea Research Part I: Oceanographic Research Papers. https://doi.org/10.1016/j.dsr.2007.04.010.
- Ridgway, K. R., & Condie, S. A. (2004). The 5500-km-long boundary flow off western and southern Australia. Journal of Geophysical Research, 109, C04017. https://doi.org/10.1029/2003JC001921.
- Ridgway, K. R., & Dunn, J. R. (2003). Mesoscale structure of the mean East Australian current system and its relationship with topography. Progress in Oceanography, 56, 189-222.
- Ridgway, K. R., & Dunn, J. R. (2007). Observational evidence for a southern hemisphere oceanic 'Supergyre'. Geophysical Research Letters, 34, L13612. https://doi.org/10.1029/2007GL030392.
- Ridgway, K. R., Dunn, J. R., & Wilkin, J. L. (2002). Ocean interpolation by four-dimensional weighted least squares—Application to the waters around Australasia. Journal of Atmospheric and Oceanic Technology, 19(9), 1357–1375.
- Roberts, C. M., McClean, C. J., Veron, J. E. N., Hawkins, J. P., Allen, G. R., McAllister, D. E., et al. (2002). Marine biodiversity hotspots and conservation priorities for tropical reefs. Science. https://doi.org/10.1126/science.1067728.
- Rochford, D. J. (1969). Seasonal interchange of high and low salinity surface waters off south-West Australia. Technical Paper Australia: Division of  $Fisheries \ and \ Oceanography, \ CSIRO. \ http://hdl.handle.net/102.100.100/321788? index = 1.$
- Roemmich, D., & Gilson, J. (2009). The 2004–2008 mean and annual cycle of temperature, salinity, and steric height in the global ocean from the Argo Program. Progress in Oceanography, 82(2), 81-100. https://doi.org/10.1016/j.pocean.2009.03.004.
- Rosell-Fieschi, M., Rintoul, S. R., Gourrion, J., & Pelegrí, J. L. (2013). Tasman leakage of intermediate waters as inferred from Argo floats. Geophysical Research Letters, 40(20), 5456-5460. https://doi.org/10.1002/2013GL057797.
- Rousselet, L., Cessi, P., & Forget, G. (2020). Routes of the upper branch of the Atlantic meridional overturning circulation according to an ocean state estimate. Geophysical Research Letters, 47(18). https://doi.org/10.1029/2020GL089137.
- Roxy, M. K., Ritika, K., Terray, P., & Masson, S. (2014). The curious case of Indian Ocean warming. Journal of Climate, 27(22), 8501–8509. https://doi. org/10.1175/JCLI-D-14-00471.1.
- Roxy, M. K., Saranya, J. S., Modi, A., Anusree, A., Cai, W., Resplandy, L., ... Frölicher, T. L. (2024). Chapter 20: Future projections for the tropical Indian Ocean. In C. C. Ummenhofer, & R. R. Hood (Eds.), The Indian Ocean and its role in the global climate system (pp. 469-482). Amsterdam: Elsevier. https://doi.org/10.1016/B978-0-12-822698-8.00004-4.
- Rühs, S., Durgadoo, J. V., Behrens, E., & Biastoch, A. (2013). Advective timescales and pathways of Agulhas leakage. Geophysical Research Letters, 40(15), 3997-4000. https://doi.org/10.1002/grl.50782.
- Rühs, S., Schwarzkopf, F. U., Speich, S., & Biastoch, A. (2019). Cold vs. warm water route-sources for the upper limb of the Atlantic meridional overturning circulation revisited in a high-resolution ocean model. Ocean Science, 15(3), 489-512. https://doi.org/10.5194/os-15-489-2019.

- Sallée, J.-B., Wienders, N., Speer, K., & Morrow, R. (2006). Formation of subantarctic mode water in the southeastern Indian Ocean. Ocean Dynamics, 56, 525-542. https://doi.org/10.1007/s10236-005-0054-x.
- Saville-Kent, W. (1897). The Naturaliste in Australia. New York: Chapman and Hall. 302 pp.
- Schodlok, M. P., Tomczak, M., & White, N. (1997). Deep sections through the South Australian Basin and across the Australian-Antarctic discordance. Geophysical Research Letters, 24(22), 2785–2788.
- Schouten, M. W., de Ruijter, W. P. M., & van Leeuwen, P. J. (2002a). Upstream control of Agulhas ring shedding. Journal of Geophysical Research, 107 (10.1029)
- Schouten, M. W., de Ruijter, W. P. M., van Leeuwen, P. J., & Dijkstra, H. (2002b). An oceanic teleconnection between the equatorial and southern Indian Ocean. Geophysical Research Letters, 29(16), 51-59.
- Schulze Chretien, L. M., & Speer, K. (2018). A deep eastern boundary current in the Chile Basin. Journal of Geophysical Research: Oceans, 124, 27-40. https://doi.org/10.1029/2018JC014400.
- Schwarzkopf, F. U., Biastoch, A., Böning, C. W., Chanut, J., Durgadoo, J. V., Getzlaff, K., et al. (2019). The INALT family—A set of high-resolution nests for the Agulhas current system within global NEMO Ocean/sea-ice configurations. Geoscientific Model Development, 12(7), 3329-3355. https://doi. org/10.5194/gmd-12-3329-2019.
- Sen Gupta, A. R., Ganachaud, A., McGregor, S., Brown, J. N., & Muir, L. (2012). Drivers of the projected changes to the Pacific Ocean equatorial circulation. Geophysical Research Letters, 39. https://doi.org/10.1029/2012GL051447.
- Sen Gupta, A., McGregor, S., Van Sebille, E., Ganachaud, A., Brown, J. N., & Santoso, A. (2016). Future changes to the Indonesian Throughflow and Pacific circulation: The differing role of wind and deep circulation changes. Geophysical Research Letters, 43(4), 1669–1678. https://doi.org/10.1002/ 2016GL067757.
- Sen Gupta, A., Santoso, A., Taschetto, A. S., Ummenhofer, C. C., Trevena, J., & England, M. H. (2009). Projected changes to the Southern Hemisphere Ocean and sea ice in the IPCC AR4 climate models. Journal of Climate, 22(11), 3047–3078. https://doi.org/10.1175/2008JCLI2827.1.
- Smith, R. L., Huyer, A., Godfrey, J. S., & Church, J. A. (1991). The Leeuwin current off Western Australia, 1986–1987. Journal of Physical Oceanography, 21, 323-345. https://doi.org/10.1175/1520-0485(1991)021<0323:TLCOWA>2.0.CO;2.
- Song, Q., & Gordon, A. L. (2004). Significance of the vertical profile of Indonesian Throughflow transport on the Indian Ocean. Geophysical Research Letters, 31, L16307. https://doi.org/10.1029/2004GL020360.
- Speich, S., Blanke, B., & Cai, W. (2007). Atlantic meridional overturning circulation and the southern hemisphere supergyre. Geophysical Research Letters, 34, 1-5. https://doi.org/10.1029/2007GL031583.
- Speich, S., Blanke, B., de Vries, P., Drijfhout, S., Doos, K., Ganachaud, A., & Marsh, R. (2002). Tasman leakage- A new route in the global ocean conveyor belt. Geophysical Research Letters, 29(10), 51-55.
- Sprintall, J., Gordon, A. L., Koch-Larrouy, A., Lee, T., Potemra, J. T., Pujiana, K., & Wijffels, S. J. (2014). The Indonesian seas and their role in the coupled ocean-climate system. Nature Geoscience. https://doi.org/10.1038/NGEO2188.
- Sprintall, J., Wijffels, S. E., Molcard, R., & Jaya, I. (2009). Direct estimates of the Indonesian Throughflow entering the Indian Ocean: 2004-2006. Journal of Geophysical Research, Oceans, 114. https://doi.org/10.1029/2008JC005257.
- Stellema, A., Sen Gupta, A., & Taschetto, A. S. (2019). Projected slow down of South Indian Ocean circulation. Scientific Reports, 9(1), 1–15. https://doi. org/10.1038/s41598-019-54092-3.
- Sun, C., Feng, M., Matear, R. J., Chamberlain, M. A., Craig, P., Ridgway, K. R., & Schiller, A. (2012). Marine downscaling of a future climate scenario for Australian boundary currents. Journal of Climate, 25(8), 2947–2962. https://doi.org/10.1175/JCLI-D-11-00159.1.
- Sun, S., & Thompson, A. F. (2020). Centennial changes in the Indonesian Throughflow connected to the Atlantic meridional overturning circulation: The ocean's transient conveyor belt. Geophysical Research Letters, 47, 1-9. https://doi.org/10.1029/2020GL090615.
- Susanto, R. D., Ffield, A., Gordon, A. L., & Adi, T. A. (2012). Variability of the Indonesian throughflow within Makassar Strait 2004-2009. Journal of Geophysical Research, 117, C09013.
- Susanto, R. D., Moore, T. S., & Marra, J. (2006). Ocean color variability in the Indonesian seas during the SeaWiFS era. Geochemistry, Geophysics, Geosystems. https://doi.org/10.1029/2005GC001009.
- Swart, N. C., & Fyfe, J. C. (2012). Observed and simulated changes in the Southern Hemisphere surface westerly wind-stress. Geophysical Research Letters, 39, L16711. https://doi.org/10.1029/2012GL052810.
- Talley, L. D. (2013a). Closure of the global overturning circulation through the Indian, Pacific, and southern oceans: Schematics and transports. Oceanography, 26, 80-97. https://doi.org/10.5670/oceanog.2011.65.
- Talley, L. D. (2013b). In I. N. M. Sparrow, P. Chapman, & J. Gould (Eds.), Hydrographic atlas of the World Ocean circulation experiment (WOCE). Volume 4: Indian Ocean. Southampton, UK: International WOCE Project Office.
- Talley, L. D., Pickard, G. L., Emery, W. J., & Swift, J. H. (2011). Descriptive physical oceanography: An introduction (6th ed.). Academic Press, Elsevier Ltd. 983pp.
- Talley, L. D., & Sprintall, J. (2005). Deep expression of the Indonesian Throughflow: Indonesian intermediate water in the south equatorial current. Journal of Geophysical Research, C: Oceans, 110(10). https://doi.org/10.1029/2004JC002826.
- Tamsitt, V., Abernathey, R. P., Mazloff, M. R., Wang, J., & Talley, L. D. (2018). Transformation of deep water masses along Lagrangian upwelling pathways in the Southern Ocean. Journal of Geophysical Research: Oceans, 123, 1994–2017. https://doi.org/10.1002/2017JC013409.
- Tamsitt, V., Drake, H., Morrison, A., Talley, L. D., Dufour, C., Gray, A., et al. (2017). Spiraling up: Pathways of global deep water from the deep ocean to the surface of the Southern Ocean. Nature Communications, 8, 172.

- Tamsitt, V., Talley, L. D., & Mazloff, M. R. (2019). A deep eastern boundary current carrying Indian deep water south of Australia. Journal of Geophysical Research: Oceans, 124(3), 2218–2238. https://doi.org/10.1029/2018JC014569.
- Thompson, R. O. R. Y. (1984). Observations of the Leeuwin current off Western Australia. Journal of Physical Oceanography, 14, 623-628. https://doi. org/10.1175/1520-0485(1984)014<0623:OOTLCO>2.0.CO;2.
- Thompson, R. O. R. Y. (1987). Continental-shelf-scale model of the Leeuwin current. Journal of Marine Research, 45(4), 813–827. https://doi.org/ 10.1357/002224087788327190.
- Toole, J. M., & Warren, B. A. (1993). A hydrographic section across the subtropical South Indian Ocean. Deep Sea Research, Part 1, 40, 1973–2019.
- Tozuka, T., Dong, L., Han, W., Lengainge, M., & Zhang, L. (2024). Chapter 10: Decadal variability of the Indian Ocean and its predictability. In C. C. Ummenhofer, & R. R. Hood (Eds.), The Indian Ocean and its role in the global climate system (pp. 229–244). Amsterdam: Elsevier. https://doi.org/10. 1016/B978-0-12-822698-8.00014-7.
- Tsugawa, M., & Hasumi, H. (2010). Generation and growth mechanism of the Natal pulse. Journal of Physical Oceanography, 40, 1597-1612.
- Tun, K., Chou, L. M., Cabanban, A., Tuan, V. S., Yeemin, T., Suharsono, et al. (2004). Status of coral reefs, coral reef monitoring and management in Southeast Asia, 2004. In Status of Coral Reefs of the World: 2004—Volume 1.
- Ummenhofer, C. C., Geen, R., Denniston, R. F., & Rao, M. P. (2024). Chapter 3: Past, present, and future of the South Asian monsoon. In C. C. Ummenhofer, & R. R. Hood (Eds.), The Indian Ocean and its role in the global climate system (pp. 49-78). Amsterdam: Elsevier. https://doi.org/10.1016/B978-0-12-
- Ummenhofer, C. C., Murty, S. A., Sprintall, J., Lee, T., & Abram, N. (2021). Decadal to centennial Indian Ocean heat and freshwater changes in a regional context. Nature Reviews Earth and Environment, 2, 525-541. https://doi.org/10.1038/s43017-021-00192-6.
- Van Aken, H. M., Punjanan, J., & Saimima, S. (1988). Physical aspects of the flushing of the east Indonesian basins. Netherlands Journal of Sea Research, 22(4), 315-339. https://doi.org/10.1016/0077-7579(88)90003-8.
- Van Aken, H. M., Van Veldhoven, A. K., Veth, C., De Ruijter, W. P. M., Van Leeuwen, P. J., Drijfhout, S. S., et al. (2003). Observations of a young Agulhas ring, Astrid, during MARE in March 2000. Deep Sea Research Part II: Topical Studies in Oceanography, 50(1), 167–195. https://doi. org/10.1016/S0967-0645(02)00383-1.
- van Bennekom, A. J. (1988). Deep-water transit times in the eastern Indonesian basins, calculated from dissolved silica in deep and interstitial waters. Netherlands Journal of Sea Research. https://doi.org/10.1016/0077-7579(88)90004-X.
- van Bennekom, A. J., & Muchtar, M. (1988). Reactive phosphate in the eastern Indonesian seas. Netherlands Journal of Sea Research. https://doi.org/ 10.1016/0077-7579(88)90006-3.
- Van Sebille, E., England, M. H., Zika, J. D., & Sloyan, B. M. (2012). Tasman leakage in a fine-resolution ocean model. Geophysical Research Letters, 39, L06601. https://doi.org/10.1029/2012GL051004.
- Van Sebille, E., Sprintall, J., Schwarzkopf, F. U., Sen Gupta, A., Santoso, A., England, M. H., et al. (2014). Pacific-to-Indian Ocean connectivity: Tasman leakage, Indonesian Throughflow, and the role of ENSO. Journal of Geophysical Research: Oceans, 119(2). https://doi.org/10.1002/2013JC009525.
- Vidya, P. J., Ravichandran, M., Subeesh, M. P., Chatterjee, S., & N.M. (2020). Global warming hiatus contributed weakening of the Mascarene high in the Southern Indian Ocean. Scientific Reports, 10, 3255. https://doi.org/10.1038/s41598-020-59964-7.
- Weijer, W., Cheng, W., Garuba, O. A., Hu, A., & Nadiga, B. T. (2020). CMIP6 models predict significant 21st century decline of the Atlantic meridional overturning circulation. Geophysical Research Letters, 47, e2019GL086075. https://doi.org/10.1029/2019GL086075.
- Weijer, W., & van Sebille, E. (2014). Impact of Agulhas leakage on the Atlantic overturning circulation in the CCSM4. Journal of Climate, 27, 101–110.
- Wijffels, S., & Meyers, G. (2004). An intersection of oceanic waveguides: Variability in the Indonesian Throughflow region. Journal of Physical Oceanography. https://doi.org/10.1175/1520-0485(2004)034<1232:AIOOWV>2.0.CO.
- Wijffels, S. E., Meyers, G. M., & Godfrey, J. S. (2008). A 20-Yr average of the Indonesian Throughflow: Regional currents and the interbasin exchange. Journal of Physical Oceanography, 38, 1965-1978.
- Woo, M., & Pattiaratchi, C. (2008). Hydrography and water masses of the western Australian coast. Deep Sea Research, 55, 1090–1104.
- Wood, E. J. F. (1954). Dinoflagellates in Australian waters. Australian Journal of Marine & Freshwater Research, 5, 171-351.
- Wyrtki, K. (1971). Oceanographic atlas of the international Indian Ocean expedition. Washington, D.C.: National Science Foundation. 531 pp.
- Wyrtki, K. (1987). Indonesian Throughflow and the associated pressure gradient. Journal of Geophysical Research, 92, 12941–12946.
- Xie, T., Newton, R., Schlosser, P., Du, C., & Dai, M. (2019). Long-term mean mass, heat and nutrient flux through the Indonesian seas, based on the tritium inventory in the Pacific and Indian oceans. Journal of Geophysical Research: Oceans, 124(6), 3859-3875. https://doi.org/10.1029/2018JC014863.
- Xu, T., Li, S., Hamzah, F., Setiawan, A., Susanto, R. D., Cao, G., & Wei, Z. (2018). Intraseasonal flow and its impact on the chlorophyll-a concentration in the Sunda Strait and its vicinity. Deep-Sea Research Part I: Oceanographic Research Papers. https://doi.org/10.1016/j.dsr.2018.04.003.
- Yamagami, Y., Tozuka, T., & Qiu, B. (2019). Interannual variability of the Natal pulse. Journal of Geophysical Research: Oceans, 124(12), 9258-9276. https://doi.org/10.1029/2019JC015525.
- Zhang, Y., Feng, M., Du, Y., Phillips, H. E., Bindoff, N. L., & McPhaden, M. J. (2018). Strengthened Indonesian Throughflow drives decadal warming in the Southern Indian Ocean. Geophysical Research Letters, 45(6167), 6175. https://doi.org/10.1029/2018GL078265.
- Zheng, Q. (2018). Water mass and velocity structure of the subsurface westward flows in the South Indian Ocean. (Honours thesis). University of Tasmania. 50 pp.